Transportation Research Part D 116 (2023) 103617

Contents lists available at ScienceDirect

Transportation Research Part D

journal homepage: www.elsevier.com/locate/trd

Deployment optimization of battery swapping stations accounting for taxis' dynamic energy demand

Tian-yu Zhang [a], En-jian Yao [a,*], Yang Yang [a], Long Pan [a], Cui-ping Li [d], Bin Li [b], Feng Zhao [c]

[a] Key Laboratory of Transport Industry of Big Data Application Technologies for Comprehensive Transport, Beijing Jiaotong University, Beijing, China
[b] The Research Institute of Highway Ministry of Transport, Beijing, China
[c] The Tianjin Intelligent Traffic Operation Monitoring Center, Tianjin, China
[d] Automotive Data of China (Tianjin), Co., Ltd, Tianjin, China

ARTICLE INFO

Keywords:
Battery swapping
Electric taxi
Battery swapping station
Station planning
Multi-agent-based microscopic swapping behavior simulation
Dynamic demand

ABSTRACT

Current research on battery swapping stations (BSSs) deployment problems overlooks the influence of BSS layouts on the daily performance of battery swapping taxis (BSTs). This study aims to propose a BSS deployment optimization model to guarantee taxi transport capacity. To this end, the dynamic swapping demands of BSTs are predicted by modeling battery swapping behavior, reconstructing trip chain, and simulating BSS operation. Furthermore, BSSs' deployment is optimized to minimize the swapping loss time. Using the daily trajectory data of 9862 taxis in Tianjin, we set up six scenarios to elucidate the trade-off among the layout and service level, the transport capacity, and the environmental efficiency. The optimal layout ensures 98.1% of the taxi transport capacity and reduces carbon emissions by 44.09%. The employed behavioral model enhances the network equilibrium from 0.33 to 0.067. Finally, the roles of driving range and charging speed in attracting and assigning energy demand are revealed.

1. Introduction

With high energy conversion efficiency and zero pollution in driving, taxis electrification has an outsized influence on alleviating the petroleum crisis and reducing carbon emissions in urban transportation (Bauer et al., 2018; World Economic Forum, 2021). The taxi electrification process has been promoted in many cities worldwide (Zhou et al., 2021). By the end of 2020, the number of taxis in China was 1.394 million (MOT, 2021). Due to operational characteristics of taxis, the development of taxi electrification is restricted by energy replenishment efficiency. Compared with the public fast charging mode exceeding 30 min, the depleted battery swapping process can be completed within three minutes in the battery swapping station (BSS) (Ahmad et al., 2020; Yang et al., 2021). The battery swapping mode (BSM) dramatically lessens the electric vehicle (EV) energy supplement time and could substantially save urban land resources as no parking space is required (Liang et al., 2021). In recent years, the BSM has been quickly developed in China (The government of China, 2020). As of December 2020, the number of BSSs has reached 555 in China (ASKCI Consulting Co, 2020). Aulton, the world's largest commercial BSS operator, plans to build 5,000 BSSs in 100 cities by 2025 (Aulton, 2021).

One vital prerequisite to promoting battery swapping taxi (BST) development is the appropriate BSS deployment (Cilio and Babacan, 2021; Yang et al., 2021). The reliable estimation of energy demand is fundamental for energy infrastructure deployment

* Corresponding author.
E-mail address: enjyao@bjtu.edu.cn (E.-j. Yao).

https://doi.org/10.1016/j.trd.2023.103617
Received 9 October 2022; Received in revised form 8 January 2023; Accepted 14 January 2023
Available online 24 January 2023

(Zhang et al., 2022). Due to the lack of actual operation data of BSS and BST, the most existing research on BSS deployment is model-based schemes with assumed energy demand (Wu et al., 2018; An et al., 2020). Until now, some investigators have predicted the battery swapping demand based on the global positioning system (GPS) data from gasoline-powered cars (Bai et al., 2019; Wang et al., 2021). They extracted the static point message, such as the vehicle's dwell time and region's dwell count, to estimate them as energy demand. However, there are some limitations to battery swapping demand estimation in existing BSSs' deployment, as itemized in the following: (i) in model-based schemes, the assumed energy demand lacks the consideration of actual traffic network, land use, and travel behavior (Zeng et al., 2019); (ii) in GPS-based schemes, the use of taxis' dwell characters as energy demand seems irrational because there are many long-time dwell events in the daily operation of taxis, such as napping, eating, and changing shifts; (iii) in existing estimations of swapping demand, the impact of BSS layouts on the daily operation of BSTs is ignored.

In the BSM, the daily trip chain of taxis could be altered by the battery swapping event generated during the trip. Influenced by range anxiety, BST drivers should check their energy demands at the end of each passenger order in the daily operation. The taxi with swapping demand would detour to a BSS and accept battery swapping service. Subsequently, the battery swapping activity, including detouring, queueing, and swapping processes, affects the response of subsequent orders, thus changing the daily trip chain of taxis. While the length of battery swapping activity's occupancy time is affected by the deployment of the BSS network, that is, the station's quantity, location, and level. In light of this issue, this paper aims to respond to the following three questions for the BSS planning:

(1) When and where the taxi driver makes the swapping demand in the BSS network?

(2) How does the layout of BSS affect the daily trip chain of taxis?

(3) How to deploy a BSS network to guarantee the transport capacity of the taxi industry?

To respond to these crucial queries, based on the behavioral modeling and multi-agent simulation, a deployment model for multi-level BSSs with a precise prediction of the dynamic energy demand is established. Specifically, the travel mechanism of BST drivers is revealed by modeling the decision-making of users on swapping demand and BSS choice. Then, a multi-agent-based microscopic swapping behavior simulation is proposed to construct the dynamic interactions between taxis, passengers, and BSSs, and to capture the dynamic battery swapping demands. Furthermore, the locations and levels of BSSs are appropriately optimized to maximize the effective operation time of taxis. A genetic algorithm (GA) incorporating the agent-based simulation algorithm is designed to analyze the proposed deployment model. By employing the GPS data of the taxi fleet in Tianjin, the trade-offs among the layout of BSS and the system's level of service (LOS), BSTs' transport capacity, and environmental efficiency are methodically examined in six scenarios. Additionally, the sensitivity analyses of technology development to the energy demand generation of users and operations of BSSs are performed.

The paper is organized as follows. In section 2, the literature is reviewed, and the main contributions are explained. In section 3, the BST's trip chain, nomenclature, and framework are expressed. In section 4, the methodology is systematically proposed. In section 5, a case study is researched. In the last section, the major research findings and further research are outlined.

2. Literature review

2.1. EV energy efficiency

In recent years, in order to promote transportation electrification, many researchers have taken electric vehicles as the subject to improve their energy saving and emission reduction benefits from different fields. The first field is about EV driving behavior. Researchers optimize EV drivers' eco-driving strategy to avoid aggressive acceleration, deceleration, and long-time idling (Gao et al., 2019; Ma et al., 2021). The second field is about the deployment of charging/battery-swapping infrastructures. Planners guarantee the efficiency of EV charging or battery swapping by rationalizing the location and capacity of these facilities (Zhang et al., 2022). The third field is about the power structure. Governments are promoting power supply-side transformation by reducing the proportion of traditional thermal power generation, and gradually promoting green power generation, from sources such as wind, photovoltaic, and nuclear (Bogdanov et al., 2021).

2.2. EV travel behavior analysis

As soon as a new type of energy supply infrastructure or an operation mode is generated, the travel behaviors of drivers, such as route choice (Yang et al., 2016) and energy choice (Chaudhari et al., 2018), are influenced, and thereby their corresponding trip chains change. As a result, exploring the mechanism of BSTs' travel behavior is the basis for reconstructing the trip chains and estimating the energy demands in the BSM.

In recent years, the travel behavior of EVs in the presence of charging station layouts has received much attention (Hu Zhang et al., 2013; Oda et al., 2018). Based on the GPS trajectory dataset of taxis, Hu et al., 2018 evaluated the feasibility of EVs by examining the influence of charging stations on the travel patterns of taxis. Considering the users' risk attitudes, Pan et al., 2019 modeled the charging choice behavior of EVs by establishing a hybrid choice model (HCM). In a stated preference (SP) survey of 505 EV drivers, Ashkrof et al., 2020 explored their route choice and charging preference via a mixed logit (ML) model. These travel behavior models reveal the linkage between users' travel and energy demand and the traffic network and charging station status.

However, existing explorations regarding the effects of travel behavior and energy preference of taxi drivers on the BSS network are still insufficient. The energy decision-making mechanisms of vehicles are dissimilar in the presence of various energy-supplied modes (Rao et al., 2018) and different vehicle operational attributes (Zhang et al., 2016; Tang et al., 2020). On the one hand, compared with the charging mode, the energy replenishment process of the vehicle and the battery is separated in BSSs. The charging time, for

example, is a key factor that affects the choice of charging stations for EV drivers (Sun et al., 2016). While for BSTs, the charging time is only three minutes and is less significant. On the other hand, the sensitivity of taxi drivers to energy demand factors differs from private vehicles due to their operational characteristics, such as working time, shift modes, and dwell patterns (Nie, 2017). Hence, exploring the BST's travel behavior plays an essential and noticeable role in the BSS infrastructure's deployment.

2.3. Facility location problems for charging station

The facility location problems attempt to plan the infrastructure's location (Zeng et al., 2019), capacity (Yang et al., 2017), and type (An et al., 2020). The conventional location simulations include node-based and flow-based location modeling.

In node-based location modeling, the demand is aggregated into the abstract grid and assigned to the stations (Tu et al., 2016; Hu et al., 2019; Yang et al., 2021). However, the vehicle's travel process in the network is ignored or simplified. The node-based location model does not handle the BSS location problem for BSTs. This is mainly because of the fact that the battery swapping demand of BSTs mostly occurs during the trip, instead of making a trip only for battery swapping (Jung et al., 2014). In the flow-based location model, demand refers to the traffic flow along the travel network (Dong et al., 2014; He et al., 2018). The flow-based location model can capture the processes of users' route choice, system service, and flow transmission (Huang and Kockelman, 2020; Zhang et al., 2022). However, the model only takes into account the vehicle's single itinerary, and the trip chain constituted with continuous trips could not be effectively modeled.

Because of the inherent complexity of the problem and the constraints of the location model, the complex behaviors of BSTs and the operational processes of BSSs cannot be modeled and integrated into the conventional location models (Yang et al., 2020). As a microscopic simulation model, agents can dynamically learn from their environments and accordingly respond in multi-agent simulations (Klein et al., 2020). Multi-agent simulations have excellent micro simulation performances for transportation systems since these calculations can establish the dynamic interaction between vehicle, traffic network, and grid network (Pagani et al., 2019; Jahn et al., 2020), and can capture the dynamic energy demands of users subjected to an equilibrium assignment (Wei et al., 2017).

2.4. Research motivations, and contributions

As reviewed above, most researchers optimize the infrastructure deployment based on the static or dynamic traffic demand during a single trip, which ignores the impact of the infrastructure layout on drivers' travel behaviors as well as the variations of the daily trip change of taxis. Hence, this paper is aimed to propose a deployment model for multi-level BSSs with a precise estimation of dynamic energy demand. The main contributions of this paper could be briefly displayed as follows:

(1) The travel behaviors of BSTs, including the decision-making of swapping demand and the choice of BBS, are modeled based on the stochastic utility theory. The SP survey is first introduced for various battery swapping scenarios of BSTs. Furthermore, the mathematical models reveal the mechanism of travel behaviors of BSTs and provide a theoretical basis for the energy demand estimation of BSTs.
(2) This paper develops a multi-agent-based dynamical swapping demand estimation model (MDSDEM) to capture the dynamic battery swapping demand. With the travel behavior modeling and multi-agent-based simulation, the MDSDEM establishes the dynamic interaction between BSTs, passenger orders, and BSSs. According to the real-time network status, the BST drivers dynamically decide on their battery swapping demand and reconstruct their trip chain embedding the battery swapping event.
(3) In the proposed deployment optimization model, the supply and demand of facility service and loads are matched full-time through the integrated modeling of operation and planning. At the operation level, the MDSDEM realizes a comprehensive assessment of BSS deployment by monitoring the full-time status of BSTs, passenger orders, and BSS networks. At the planning level, the BSS deployment is optimized to guarantee the rationality of the LOS of the BSS network in the full time, even during peak periods.
(4) Aimed at lessening the impact of the BSM on the daily operation of taxis, a deployment model for optimizing BSSs' locations and levels to maximize effective taxi operation time is proposed. The trade-off between the BSS layout scale and the system's LOS, BSTs' transport capacity, and environmental efficiency is explained and discussed in a case study to determine the appropriate and economical construction. Then, the sensitivity of the driving range and charging speed are analyzed, illustrating the impact of the developed technology on the BSS market.

3. BST's trip chain, nomenclature, and framework

3.1. BST's trip chain

During the daily operational process of taxis, the battery swapping event could change the trip trajectory of BSTs. Therefore, on top of the trip chain of the gasoline taxi, the BST trip chain is abstracted to illustrate the influence of the BSM on the operation of taxis.

The trip chain of the BST is marked by four types of chains, i.e., the timing chain, location chain, state of charge (SOC) chain, and order chain. A complete trip refers to the journey from the end of the last order to the end of the current order, including the dead-heading process and the carrying process. The nth trip of the BST is represented as follows: $\langle t_{O_n}, (lon_{O_n}, lat_{O_n}), SOC_{O_n}, dd_n, path, t_{D_n}, (lon_{D_n}, lat_{D_n}), SOC_{D_n}, dc_n, rm_{D_n} \rangle$, where (lon_{O_n}, lat_{O_n}) and (lon_{D_n}, lat_{D_n}) in order represent

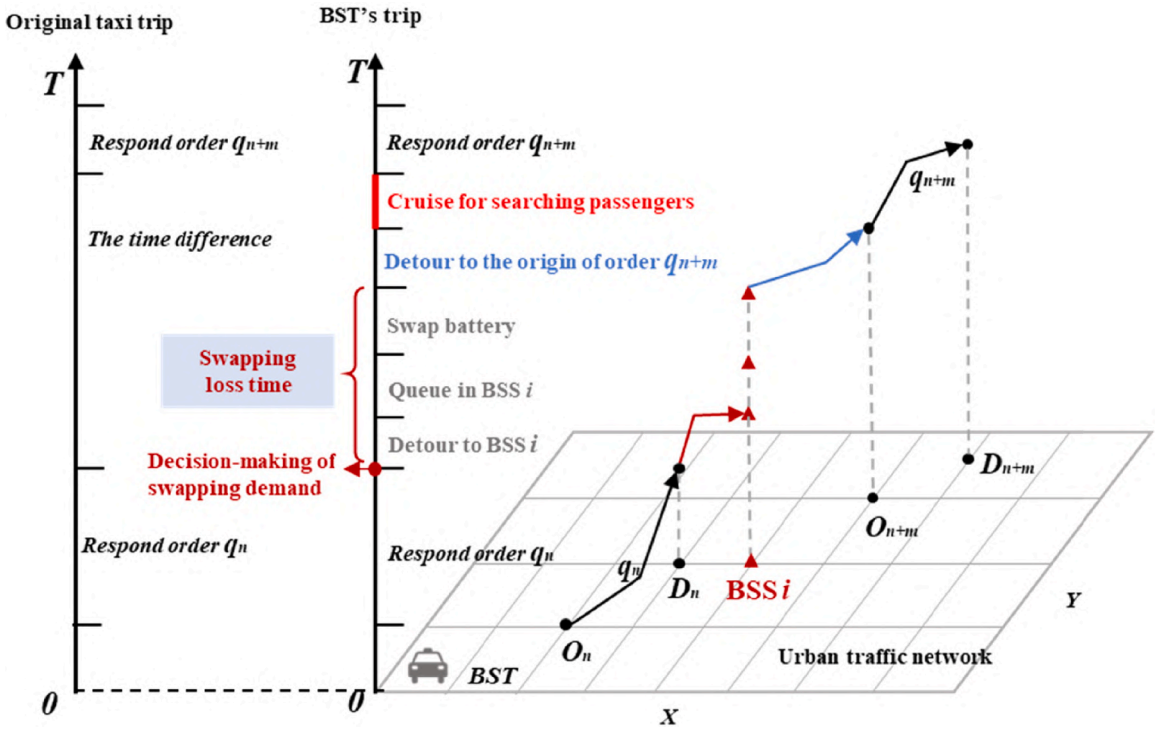

Fig. 1. Spatial-temporal pattern of BST's trip considering swapping behavior.

the location (longitude and latitude) of the origin and destination, t_{O_n} and t_{D_n} denote the entering and exiting time of passenger, SOC_{O_n} and SOC_{D_n} stand for the SOC at the origin and destination, dd_n and dc_n represents the deadhead kilometers and carrying kilometers of this order, rm_{D_n} denotes the remaining mileage of taxi at the destination, and *path* stands for the GPS trajectory of this order.

Fig. 1 illustrates the trip chain of the BST by embedding the swapping process on the gasoline taxi trajectory. To further clarify this, the swapping process includes energy demand decision-making, station choice, and battery swapping. When a taxi arrives at the destination of the order, the driver should decide whether to swap the battery. For the taxi without a swap demand, the driver will follow its original trajectory to complete the following order; otherwise, the taxi driver should choose a station to swap the battery. Subsequently, after detouring, queueing, and swapping, the taxi leaves the BSS with a fully charged battery and detours to pick up the next passenger according to the original order messages.

3.2. Nomenclature

The notation of sets and variables are shown as follows:

Sets	
I	The set of candidate BSSs,$i \in I$
X	The set of taxis,$x \in X$
X_i	The set of taxis at candidate site$i$,$x \in N_i$
B_i	The number of batteries at candidate site$i$,$b \in B_i$
R_i	The number of swapping robots at candidate site$i$,$r \in R_i$
Q_x	The order demand of taxi$x$,$q_x \in Q_x$
T	The set of time,$t \in T$
$N_{i,t}$	The set of taxis in station i at time t
Parameters	
$RM_{\min}$	The lower pound of remaining mileage
$d_{\max}$	The driving range of BST
$SOC^{\exp}$	The expected SOC for drivers
r	The radius of the Earth, which is 6371 km
cs_i	The charging speed of battery of station i
C_1,C_2	The unit construction costs of level 1 BSS and level 2 BSS
f_i	The unit swapping cost of BSS at candidate site i
C	The limitation of construction cost
E	The capacity of battery

(*continued on next page*)

(*continued*)

Sets	
I	The set of candidate BSSs,$i \in I$
Variables	
v_x	The average driving speed of taxi x
rm_{x,D_n}	The remaining mileage of taxi x at the destination in order n
$d_{x,n}$	The carrying kilometers of taxi x in order n
l^i_{x,D_n}	The distance from the taxix's destination in order n to station i
SOC_{x,D_n}	The status of charge of taxi x at the destination in order n
(λ_i, φ_i)	The longitude and latitude of station i
$(\lambda_{x,D_{n+1}}, \varphi_{x,D_{n+1}})$	The longitude and latitude of the destination in order n for taxi x
P^{swap}_{x,D_n}	The swapping probability of taxi x at the destination in order n
s_{x,D_n}	Binary variable, 1 indicates that taxi x swap the battery after finishing order$n$, 0 otherwise
$t^c_{x,i,t}$	The battery charging time of taxi x at station i
$SOC_{x,i,t}$	The status of charge of taxi x at station i at time t
$t^{usable,b}_{i,t}$	The idle time of battery b at station i
$t^a_{x,i,t}$	The arriving time of taxi x at station i
$t^s_{x,i,t}$	The swapping battery time of taxi x at station i
$t^{usable,r}_{i,t}$	The idle time of swapping robot r at station i
$t^e_{x,i,t}$	The leaving time of taxi x at station i
$t^w_{x,i,t}$	The waiting time of taxi x at station i
$q_{i,t}$	The queue length of station i at time t
$y^a_{i,t}$	The number of taxis arriving at station i at time t
$y^e_{i,t}$	The number of taxis leaving at station i at time t
$s_{x,i,t}$	Binary variable, 1 indicates that taxi x accepts the swapping service at station i at time$t$, 0 otherwise
$t^d_{x,i,t}$	The detour time of taxi x to station i
z_i	Binary variable, 1 indicates that a BSS is built at candidate site$i$, 0 otherwise
η_i	The level of BSS at candidate site i
$b_{i,t}$	The number of remaining available batteries at station i at time t
$r_{i,t}$	The number of idle swapping robots at station i at time t

Several definitions and assumptions are explained in the following:

Definition 1

The swapping loss time of the BST consists of the detour time, the waiting time, and the battery swapping time together.

Definition 2

The effective taxi service time is defined as the operating time of a taxi, which excludes the swapping loss time.

Assumption 1

The reassignment of lost orders due to battery swapping events is ignored.

Assumption 2

The real-time information transmission between BSTs, BSSs, and passengers can be accomplished with the developed wireless communication technology.

3.3. Framework

Based on the dynamic BST's battery swapping demand, herein, a deployment model is proposed to integrate behavioral modeling and multi-agent simulations for the urban BSS network. The detailed framework has been illustrated in Fig. 2.

The deployment model is implemented by the following steps. Initially, the swapping decision-making process and the station choice process are simulated, providing an appropriate basis for reconstructing the trip chain and estimating the energy demand. The MDSDEM is then developed to capture the dynamic swapping demand by simulating the BST's swapping behavior and the BSS network's operation, following the deployment of the BBS network. The total BSTs' detour time, waiting time, and operation time are then evaluated as the input of the BSS's deployment model. Finally, the deployment model optimizes BSSs' layout to minimize the impact of the BSM on taxi transport capacity and outputs the new solution (locations and levels of stations) into the MDSDEM until finding the best solution.

4 Methodology

4.1. Modeling the travel behavior of BST drivers

In this paper, an SP survey is conducted with taxi drivers who have swapping experience. Its main objective is to identify when they swap the battery and how they choose the swapping station. The 36 scenarios involved in the survey are designed by the D-optimal method, considering the factors of season, vehicle characteristics, station operational status, the popularity of taxi demand near the site, and other characteristics. Further, based on the stochastic utility theory, the processes of swapping decision and BSS choice are

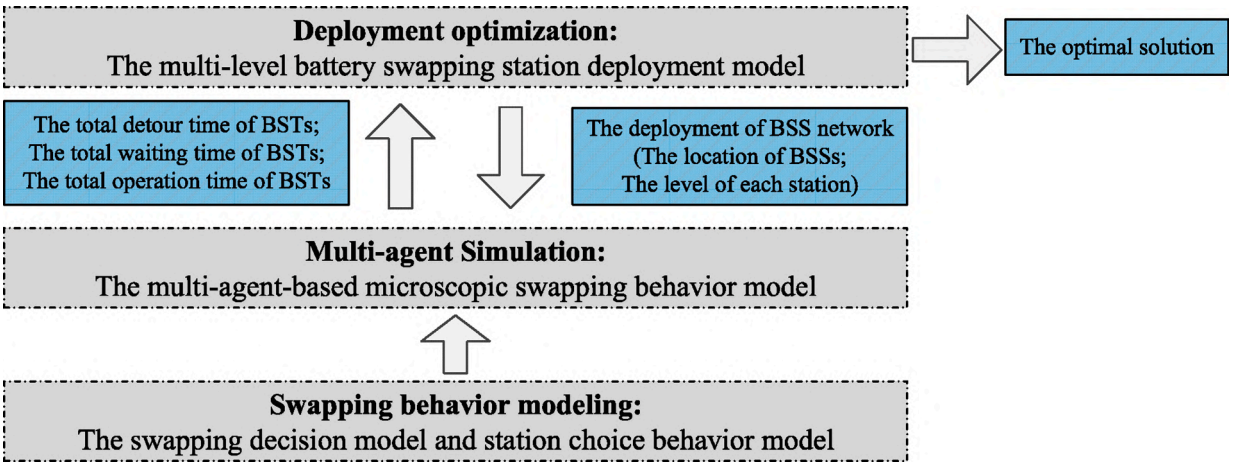

Fig. 2. The framework of the deployment model based on MDSDEM.

appropriately modeled accounting for the panel data utility, respectively. The detailed survey and behavior modeling are given in the following.

4.1.1. SP survey of BST drivers' swapping behavior

The survey scenario involves two parts: the decision-making of swapping demand and the choice of swapping station. In order to precisely examine the mechanism of BST swapping behavior, the scene design considers various factors that may affect the drivers' swapping behavior. Four essential factors are set in assessing the decision-making scenario of swapping demand, i.e., the driving range, current time, the remaining range, and season. In addition, the scenario of BSS choice is designed by six variables, including the number of available batteries, swapping price, queue length, detour distance, and popularity of taxi demand near the station. Among them, the proposed popularity of taxi demand refers to the density of passenger demand for taxis. Table 1 lists the detailed variables setting of the two scenarios.

Through combining and filtering the proposed variables, 36 scenes are designed by the D-optimal experimental design approach. The illustrative sketch of the swapping scenario has been demonstrated in Fig. 3. Meanwhile, to ensure data reliability, the questionnaire is only available to drivers with battery swapping experience, particularly taxi drivers. From August to September 2020, 627 valid samples were obtained, among which 83 % of respondents were taxi drivers, while the remaining 17 % were ride-hailing drivers.

4.1.2. Modelling swapping behavior with panel data utility

According to the stochastic utility theory, the discrete choice model with panel data utility is adopted in the present scrutiny to model the battery swapping behavior of BSTs.

In the utility function, the feature of the panel data (Thøgersen, 2006; Yáñez et al., 2011) is also an influential factor to be considered. Generally, there exists a correlation between multiple selections by the same respondent in the panel data. Furthermore, the correlation is defined as state dependence, representing positive and negative states. Hence, a particular error term is introduced to exhibit the state dependence based on the utility function of the traditional discrete choice model. The probability of the scheme selection and the utility function accounting for the panel data utility are formulated in the following form:

$$P_{in} = prob(U_{in} > U_{jn}; i \neq j, j \in A_n) = \frac{e^{V_{in}}}{\sum_{j \in A_n} e^{V_{jn}}} \tag{1}$$

$$U_{in} = V_{in} + \varepsilon_{in} + \varepsilon_{in}^{'} \tag{2}$$

Table 1
Variable setting of swapping scenarios.

Scenarios	Variable description	Unit	Variable level
The decision-making of swapping demand	Driving range	km	300; 350; 400; 450
	Time	o'clock	0–11; 11–15; 15–18; 18–24
	Remaining range	km	40; 80; 120; 150
	Season	–	spring/fall; summer/winter
The choice of swapping station	The number of available batteries	piece	1; 7; 14; 21; 28
	Swapping price	RMB/km	0.2; 0.3; 0.4
	Queue length	pcu	0; 3; 5; 8
	Detour distance	km	1; 3; 5
	The popularity of taxi demand	–	1; 2; 3; 4; 5

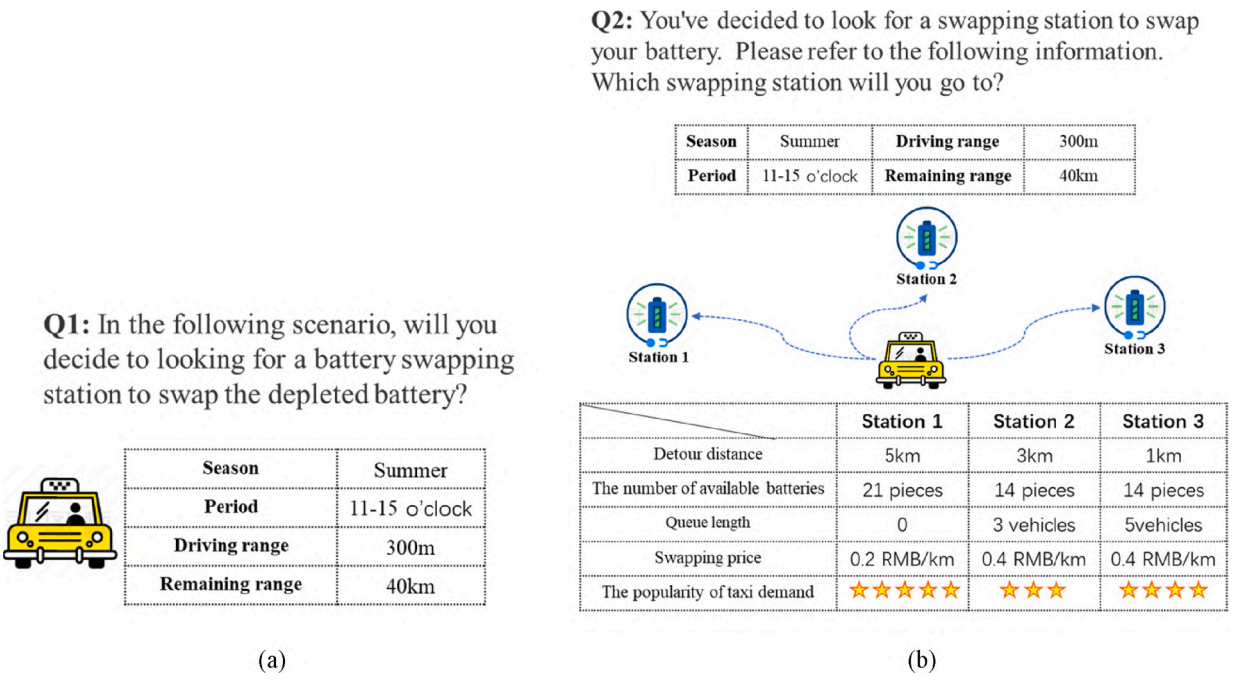

Fig. 3. An illustration of the battery swapping scenario: (a) question on whether to swap battery, (b) question on choice which station.

where P_{in} represents the probability of the i-th scheme selection for the n-th user, such that $0 < P_{in}$ *less than 1,* and $\sum P_{in} = 1$. The parameters U_{in} and V_{in} denote the utility function and the generalized utility of the i-th scheme for the n-th user, ε_{in} is the error term following the Gumbel distribution, and ε'_{in} represents the new error term that follows a normal distribution with a mean of zero, i.e., $\varepsilon'_{in} \sim N(0, \sigma_{\varepsilon'in})$.

In view of the above, the binary logit (BL) model and the multinominal nest logit (MNL) model in order are utilized to model the process of swapping demand decision-making and station choice. Meanwhile, modeling is performed with the addition of the panel data, considering the utility of panel data on model calibration. The correlations among the four understudied models have been demonstrated in Fig. 4.

The model is calibrated by the Biogeme software, and the parameters in the model are estimated by implementing the maximum likelihood estimation method. The results are provided as follows:

(1) The swapping demand decision-making

The calibration results of the swapping demand decision-making model are given in Table 2. The adjusted ρ^2 demonstrates that the model (DEMAND_DECISION 2) with panel data outperforms the basic model (DEMAND_DECISION 1). The t-value of the error term 1 is calculated to be 6.70. It indicates that the error term representing state dependence substantially affects the results of the swapping demand decision-making of BST drivers.

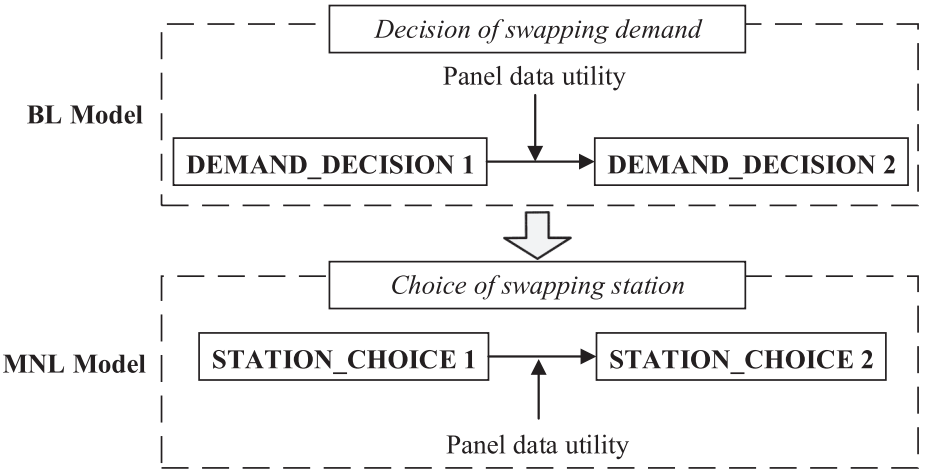

Fig. 4. Correlations among four models.

Table 2
Estimation results for BL models of the swapping demand decision.

Variables	Parameters	Estimation results (*t*-values in parentheses)	
		DEMAND_DECISION 1	DEMAND_DECISION 2
SOC (%)	soc	−6.380 (-7.710)	−9.500(-7.50)
Season (1 indicates winter, 0 otherwise)	$season$	0.427 (2.120)	0.651(2.54)
Daily average deadhead kilometers (1 indicates more than 100 km, 0 otherwise)	$d_{deadhead}$	0.476 (2.250)	0.690(1.79)
Constant	θ	2.350 (9.090)	3.500 (7.970)
Error term 1	$\sigma_1^{'}$	–	1.760(6.70)
Sample size	–	627	627
Log-likelihood	$L(\theta)$	−434.6	−434.6
Adjusted ρ^2	$\overline{\rho}^2$	0.185	0.235

In DEMAND_DECISION 2, most factors are statistically significant at the 95 % level. The SOC parameter considerably yields a negative sign, meaning the lower willingness of drivers to swap batteries with higher SOC. The season dummy variable is positive, indicating that BST drivers are more likely to swap batteries in summer or winter. This issue is essentially attributed to the fact that the exploitation of air conditioning in these two seasons causes additional consumption of vehicle SOC. The parameter of daily average deadhead kilometers reveals that the drivers who drive vehicles with more than 100 km deadhead would prefer to swap the battery.

Based on the DEMAND_DECISION 2 model, the swapping probability P_{swap} and generalized utility of the swapping demand V_{swap} are expressed by Eqs. (3) and (4).

$$P_{swap} = \frac{\exp(V_{swap})}{\exp(V_{swap}) + 1} \tag{3}$$

$$V_{swap} = 3.5 - 9.500*soc + 0.651*season + 0.690*d_{deadhead} \tag{4}$$

(5) The swapping station choice.

The estimation results of the swapping station choice model are presented in Table 3. By adding the panel data into the model, the adjusted ρ^2 enhances from 0.136 to 0.182, and the *t*-value of error term 2 is evaluated to be 5.16. They demonstrate that STATION_CHOICE 2 with panel data outperforms STATION_CHOICE 1 and that there is an apparent state dependence in drivers' selection of the BSS.

In STATION_CHOICE 2, the sign of each parameter indicates that they have different effects. The detour distance, queue length, and swapping price are negative in the BSS utility. Instead, the number of available batteries, which affects the driver's waiting time, is stated as positive. The reason is that drivers prefer stations with more available batteries instead of waiting for depleted batteries to charge. Additionally, the popularity of taxi demand near BSSs yields a positive sign. When choosing a BSS, BST drivers consider the number of passenger orders surrounding the swapping station.

Based on the STATION_CHOICE 2 model, the chosen probability P_i and the generalized utility of the i-th swapping station V_i are provided by Eqs. (5) and (6).

$$P_i = \frac{\exp(V_i)}{\sum_{j=1}^{n}\exp(V_j)} = \frac{1}{\sum_{j=1}^{n}\exp(V_j - V_i)} \tag{5}$$

$$V_i = -0.325*d_{detour,i} + 0.0529*n_{battery,i} - 0.111*l_{queue,i} - 1.020*\mathrm{cost}_i + 0.0927*pop_i \tag{6}$$

Table 3
Estimation results for MNL models of the swapping station choice.

Variables	Parameters	Estimation results (*t*-values in parentheses)	
		STATION_CHOICE 1	STATION_CHOICE 2
Detour distance (km)	$d_{detour,i}$	−0.216 (-5.870)	−0.325(-5.36)
The number of available batteries (piece)	$n_{battery,i}$	0.0321 (2.540)	0.0529(3.03)
Queue length (pcu)	$l_{queue,i}$	−0.083 (-2.540)	−0.111(-2.38)
Swapping price * 10 (RMB/km)	cost_i	−0.626 (-6.690)	−1.020(-5.59)
The popularity of taxi demand near BSS	pop_i	0.053 (1.770)	0.0927(1.83)
Error term 2	$\sigma_{2,i}^{'}$	–	1.900(5.16)
Sample size	–	435	435
Log-likelihood	$L(\theta)$	−301.52	−301.52
Adjusted ρ^2	$\overline{\rho}^2$	0.136	0.182

4.2. Multi-agent-based dynamic swapping demand estimation

4.2.1. MDSDEM framework

A simulation model named MDSDEM is developed to capture the spatio-temporal distribution of swapping demand. The framework of the MDSDEM contains three layers, i.e., the geography layer, the agent demand response layer, and the BSS network service simulation layer. The interactional relationships among these layers have been illustrated in Fig. 5.

The geographic layer serves as the base layer, providing taxi GPS trajectories, administration land-use patterns, and a BSS network in the upper layer. Based on this information, the dynamic information interaction is realized between the agent demand response layer and the BSS network service simulation layer by the following process. First, the swapping demand response mechanism of each BST is established in the middle layer. The mechanism is implemented through the agent consisting of two sub-modules, including the network status sensing module and the BST swapping demand decision-making module. Through the network status sensing module, the agent could obtain the full network information in real-time, including the order request, vehicle SOC, and BSS network status. Through combining with the BST swapping demand decision-making module, the agent decides on whether to swap the battery and which BSS to select. Next, after inputting the swapping demand information, the depleted battery charging process and the BST swapping process are simulated in the BSS network service simulation layer, respectively. Finally, the dynamic BSS network statuses (i.e., the BSS facility status, the battery status, and the BST status) are timely updated and delivered to the agent.

In MDSDEM, the BST is an adaptive agent capable of making the swapping demand decision independently by dynamically sensing the surrounding information. The agents could associate with each other, and the whole system comes to a demand equilibrium assignment through the network status sensing module (Wei et al., 2017).

In the following subsections, the three sub-models involved in the MDSDEM (i.e., Model A-1: Swapping Demand Assignment, Model A-2: Orders Response Mechanisms, and Model A-3: Service System of Multi-level Swapping Stations) are further described.

4.2.2. Model A-1: Swapping demand assignment

Using Model A-1, the deriver of BST should decide whether and where to swap the battery based on the current vehicle status, order information, and BSS network layout. In this model, the dynamic energy demand of the BST is assigned through the following three steps:

(1) The judgment of fulfilling the order.

After finishing one order, the driver first should judge whether the current SOC is sufficient for the next order's demand. Hence, Eq. (7) illustrates the condition for fulfilling the next order, which necessitates the current remaining mileage should be greater than the sum of the next order mileage, the minimum detour distance to a BSS, and the remaining mileage limitation. The remaining mileage and SOC after finishing order D_{n+1} are evaluated by utilizing Eqs. (8) and (9), respectively. As shown in Eq. (10), the detour distance is calculated by Haversine formulation based on the latitude and longitude of the passenger drop-off point and the BSS. And the detour time is calculated as Eq. (11).

$$rm_{x,D_n} \geqslant d_{x,n+1} + RM_{\min} + \min_{i \in I}(l^i_{x,D_{n+1}}) \tag{7}$$

$$rm_{x,D_{n+1}} = rm_{x,D_n} - d_{x,n+1} \tag{8}$$

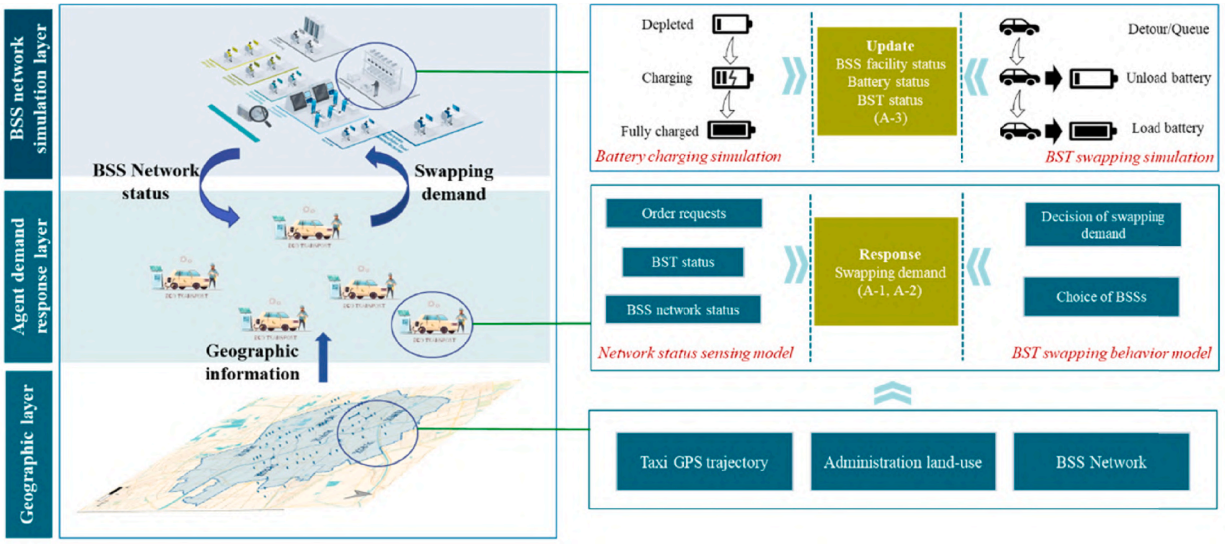

Fig. 5. MDSDEM framework.

$$SOC_{x,D_{n+1}} = SOC_{x,D_n} - d_{x,n+1}/d_{\max} \tag{9}$$

$$l^i_{x,D_{n+1}} = 2r\arcsin\left[\sqrt{\sin^2(\frac{\varphi_i - \varphi_{x,D_{n+1}}}{2}) + \cos\varphi_i \cos\varphi_{x,D_{n+1}} \sin^2(\frac{\lambda_i - \lambda_{x,D_{n+1}}}{2})}\right] \tag{10}$$

$$t^d_{x,i,t} = l^i_{x,D_{n+1}}/v_x \tag{11}$$

(2) The decision-making of energy

The decision-making of swapping battery of BST is determined by the order fulfilling condition and the demand preference of users, which is given in Eq. (12).

$$s_{x,D_n} = \begin{cases} 1, & \left[rm_{x,D_n} < d_{x,n+1} + RM_{\min} + \min_{i\in I}(l^i_{x,D_{n+1}})\right] \ or \ \left[P^{swap}_{x,D_n} \geqslant 0.5\right] \\ 0, & otherwise \end{cases} \tag{12}$$

If the above order fulfilling condition is not satisfied, BST drivers will be forced to swap the battery. Meanwhile, their preferences for swapping the battery are assessed according to the proposed swapping demand decision model. It is specifically presented as estimating the user's swapping probability, which is evaluated by Eqs. (3) and (4). Therefore, when the condition of completing the next order is unfulfilled or the swapping probability is more than 0.5, the BST driver will be assumed to swap the battery.

(3) The choice of battery swapping station

Then, the BSS choice behaviors of BSTs are simulated, and the swapping demand is assigned to a specific BSS. The detour distance, the number of available batteries, the queue length, the swapping price, and the taxi demand popularity are all factors considered in determining the chosen probability of each BSS, as exhibited by Eqs. (5) and (6). Meanwhile, the uncertainty of drivers in selecting the BSS is assumed by the roulette wheel selection method.

4.2.3. Model A-2: Orders response mechanisms

Using Model A-2, the successive passenger order response mechanism is processed. The daily trip chain of BST is reconstructed by embedding the battery swapping event, which may cause some original passenger orders to be unsatisfied. Each order is tagged with two kinds of information: execution time and travel path. This order information is extracted by pre-processing the original taxis' GPS data. The rationale is to capture the order loss caused by the swapping event after order n, as illustrated in Fig. 6.

For gasoline taxis, the original time difference between two orders represents the deadhead time, denoted by *time(Dn → On + 1)*. Affected by the swapping event, the time difference between two orders of BST's trip chain is stated as the sum of detour time from the destination in order n to i-th BBS, the waiting time, the battery swapping time, and the deadhead time from i-th BSS to the origin in order $n + m$, represented as *time'(Dn → BSS i → On + m)*. When *time'(Dn → BSS i → On + m)* is larger than the deadhead *time(Dn → On + m-1)* and less than the deadhead *time(Dn → On + m)*, the order $n + m$ is responded, and the original passenger orders between n and $n + m$ are detected as unfulfilled orders. To avoid overestimating the vehicle SOC due to the swapping event, the time difference between *time(Dn → On + m)* and *time'(Dn → BSS i → On + m)* is regarded as the cruise process for BST searching passengers. The cruise mileage is evaluated based on the daily average deadhead speed of the taxi, and the corresponding energy consumption is also included. As a result of these procedures, the corresponding order loss can be calculated, enabling the trip chain reconstruction of the BST accounting for the order response.

4.2.4. Model A-3: Service system of Multi-level swapping stations

By employing Model A-3, the battery swapping service at the BSS, involving the BST's battery swapping and the depleted battery charging, is simulated. The BSS operation process has been presented in Fig. 7.

(1) The simulation of battery swapping of BSTs

The queue system of swapping follows the FIFO rule. Upon entering the BSS, the BST lines up in the waiting lane to wait for the swapping service, as long as a robot is idle and a battery is available simultaneously. As displayed by Eq. (13), the vehicle's waiting time is determined by the earliest idle time of both the swapping robot $\min_{r\in R_i}\left\{t^{usable,r}_{i,t}\right\} - t^a_{x,i,t}$ and the available battery $\min_{b\in B_i}\left\{t^{usable,b}_{i,t}\right\} - t^a_{x,i,t}$.

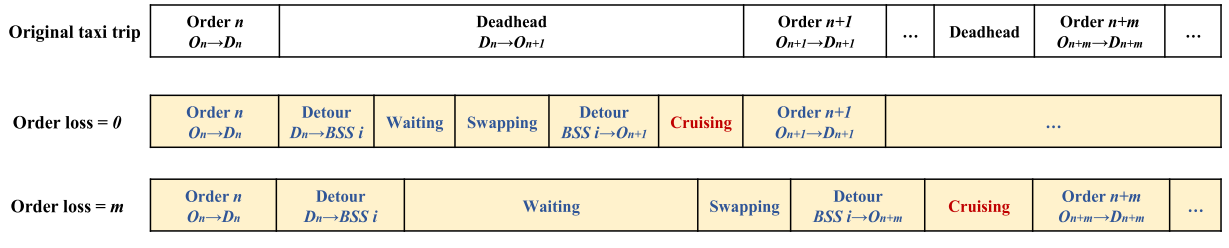

Fig. 6. The order loss caused by the swapping event.

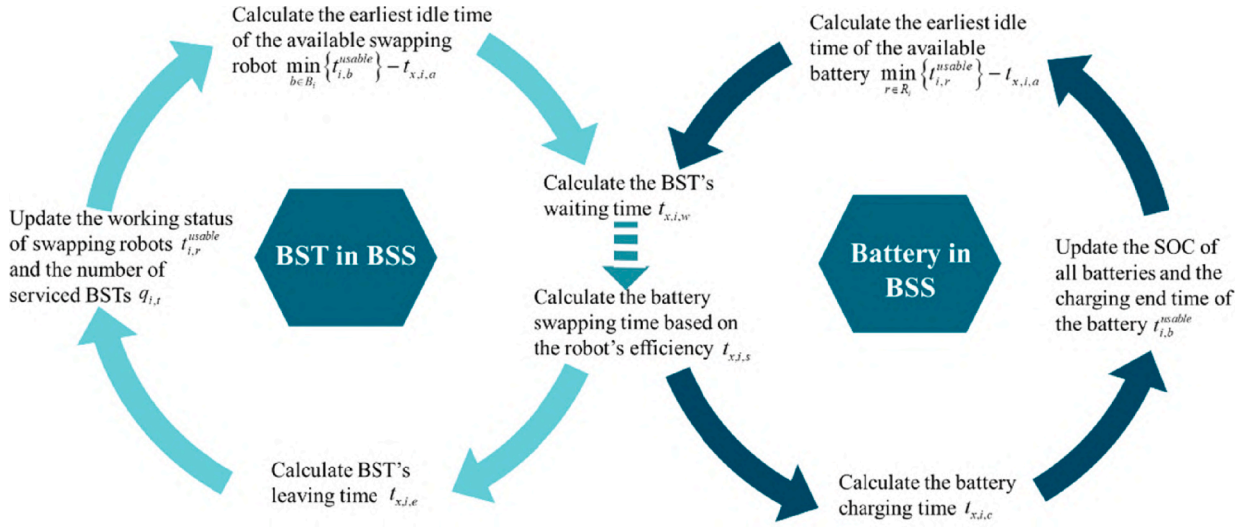

Fig. 7. Swapping service simulation at the BSS.

$$t_{x,i,t}^{w}=\max\left\{0,\min_{b\in B_i}\left\{t_{i,t}^{usable,r}\right\}-t_{x,i,t}^{a},\min_{r\in R_i}\left\{t_{i,t}^{usable,r}\right\}-t_{x,i,t}^{a}\right\} \tag{13}$$

(2) The calculations of both leaving time and battery charging time of BSTs

After finishing the swapping process, the BST would leave the BSS with a full-charged battery, and the depleted battery would be put into an available charging compartment for charging.

For BST, the dwell time in the BSS is the sum of waiting time and battery swapping time. Supplementarily, the battery swapping time is a constant, determined by the level of swapping robots. Hence, the leaving time of BST is calculated by Eq. (14)

$$t_{x,i,t}^{e}=t_{x,i,t}^{a}+t_{x,i,t}^{w}+t_{x,i,t}^{s} \tag{14}$$

For the depleted battery, the charging time depends on the remaining SOC, the expected SOC, and the charging speed, as shown in Eq. (15).

$$t_{x,i,t}^{c}=(SOC^{exp}-SOC_{x,i,t})/cs_i \tag{15}$$

(3) The update of the working status of BSSs

Last, the real-time BSS's working status of swapping robots and charging compartments, and the number of BSTs being serviced are appropriately updated.

For swapping robots, the end of service time is determined by the leaving time of the last vehicle in the station system, which is formulated by Eq. (16).

$$t_{i,t}^{usable,r}=\max_{x\in N_{i,t}}(t_{x,i,t}^{e}) \tag{16}$$

For charging compartments, the ending time of battery charging is the sum of the vehicle's arrival time, the vehicle's waiting time, the battery swapping time, and the battery charging time, as provided by Eq. (17).

$$t_{i,t}^{usable,b}=t_{x,i,t}^{a}+t_{x,i,t}^{w}+t_{x,i,t}^{s}+t_{x,i,t}^{e} \tag{17}$$

The real-time number of BSTs being serviced in the BSS is the total number of BSTs that are being swapped and waiting, as evaluated based on Eq. (18).

$$q_{i,t}=q_{i,t-1}+y_{i,t}^{a}-y_{i,t}^{e} \tag{18}$$

4.3. The deployment model and algorithms

4.3.1. Planning for multi-level BSSs

A spatio-temporal demand coverage model is proposed to optimize the BSSs deployment from two aspects: selecting locations of BSSs from the candidate sites and determining their corresponding levels.

From the perspective of ensuring the transportation capacity of taxis, reduction of the effect of swapping behavior on the original operational activities of taxis is an essential task. Furthermore, the transportation capacity of taxis is chiefly related to the effective operation time. Therefore, the optimal objective is to maximize the service time of BSTs, which is equivalent to minimizing the

swapping loss time, as formulated in Eq. (19).

$$\min \sum_{t\in T}\sum_{i\in I}\sum_{x\in X}\left(t^{d}_{x,i,t}+t^{w}_{x,i,t}+t^{c}_{x,i,t}\right)\cdot y^{a}_{i,t} \tag{19}$$

The constraints of the model are displayed in the following:

$$\sum_{i\in I} c_{\eta_i} z_i \leqslant C \ \forall z_i=\{0,1\}, \eta_i=\{1,2\} \tag{20}$$

$$\max\left(y^{a}_{i,t}\right)=z_i \ \forall i\in I, t\in T \tag{21}$$

$$\sum_{x\in X} s_{x,i,t} \leqslant \min\left(r_{i,t},\ b_{i,t}\right) \ \forall t\in T, \forall i\in I \tag{22}$$

Due to the high investment and long payback period of charging infrastructures (Burnham et al., 2017), governments or operators must decide which layout could rationally balance the construction cost and LOS. As a result, the total construction cost of BSS is constrained per given Eq. (20). The constraint of site construction is also displayed by Eq. (21), which indicates that only the candidate sites selected to build a BSS can provide a swapping service. The constraint of the real-time service capacity of the BSS is represented by Eq. (22). This relation states that the real-time number of vehicles accepting swapping services is limited by both the number of available batteries and idle swapping robots.

4.3.2. GA incorporating the agent-based simulation

Due to the complex interactions between passengers, BSTs, and facilities, the proposed BSS deployment model is an NP-hard problem. The heuristic algorithm exhibits reliable performance to find the globally optimal solutions for complex deployment problems. By beginning from natural evolutionism, GA evolves the population by selection, crossover, and mutation to find the optimal solution. So far, it has been extensively employed in solving complex location problems (Li et al., 2016).

Therefore, the GA incorporating the agent-based simulation algorithm is proposed to find the optimal solution to the BSS deployment problem. Under the BSS layout optimized by the GA approach, the agent-based simulation captures the real-time swapping demand and working status of the BSS. Subsequently, the BST's total operation time is inputted into the deployment model, and the layout is optimized until the iteration is terminated. The detailed optimization process is described in the following pseudocode.

Pseudocode of the GA incorporating the agent-based simulation Algorithm

Input: set population size P, maximum iterations M, crossover probability P_c, mutation probability P_m.
Step 1: (Generating an initial population)
Set the GA iteration $m = 1$
while $p <= P$ **do**
$p = p + 1$
Chromosome encoding.
end do //p
Return population set P^1
Step 2: (Iterative optimzation)
while $m <= M$ **do**
$m = m + 1$
for layout $\boldsymbol{y}$ in P^m
step 2.1: (MDSDEM simulation)
for time $t \in T$
for BST $x \in X$
if $STA_x = 0$ **do**
Continue the current order
elif $STA_x = 1$ **do**
Decision-making of swapping battery s_{x,D_n}
if $s_{x,D_n} = 1$ **do**
Choice the BSS i, and calculate $t^{d}_{x,i,t}, t^{w}_{x,i,t}, t^{c}_{x,i,t}$
else
Carry out the next order
elif $STA_x = 2$ **do**
Calculate order loss $loss_{x,t}$, and carry out the next order
Update vhielce status STA_x, and BSS status $t^{usable,r}_{i,t}, t^{usable,b}_{i,t}, q_{i,t}$
end for //x
end for //t
Return objective function $\sum_{t\in T}\sum_{i\in I}\sum_{x\in X}\left(t^{d}_{x,i,t}+t^{w}_{x,i,t}+t^{c}_{x,i,t}\right)\bullet y^{a}_{i,t}$
end for //$\boldsymbol{y}$
Step 2.2: (GA optimization)
Calculate the fitness $fit(\boldsymbol{y})$
Optimize Population by Selection, Crossover, Mutation P^m
end do //m
Output: best solution p_{best}

According to the BSS layout of each population, the real-time status of BSTs and BSSs in the entire network is monitored by the agent-based simulation. Based on the order status and battery status, the BST status could be divided into three types. First, the expression $STA_x = 0$ indicates that the BST is carrying passenger. The BST continues to finish the order following the original trajectory. Second, the statement $STA_x = 1$ indicates that the BST is finishing the last order. The decision-making of swapping battery s_{x,D_n} is evaluated by Eqs. (3), (4), and (11). In the case of $s_{x,D_n} = 1$, which means that BST should swap the battery, the BSS is chosen based on Eqs. (5) and (6) and the relevant detour time ($t^d_{x,i,t}$), waiting time ($t^w_{x,i,t}$), and charging time ($t^c_{x,i,t}$) are calculated by utilizing Eqs. (11), (13), and (15). Third, the expression $STA_x = 2$ represents that the BST is finishing the swapping service. The BST calculates the loss order number and starts to find the next order. After simulating the working status of all BSTs and BSSs in the whole period, the total swapping loss time $\sum_{t\in T}\sum_{i\in I}\sum_{x\in X}\left(t^d_{x,i,t} + t^w_{x,i,t} + t^c_{x,i,t}\right) \bullet y^a_{i,t}$ is calculated and outputted for the GA optimization.

5. Experiment and results

5.1. Study area description

The research is conducted in the urban center of Tianjin city, China. As illustrated in Fig. 1(a), the urban center is combined with the six districts (i.e., Hongqiao District, Heping District, Hexi District, Hedong District, Hebei District, and Nankai District). It covers 173 square kilometers, and the average resident population density is 17,370 persons/km^2.

The spatial relationships between the urban layout, taxis' trajectory, the popularity of taxi demand, and candidate BSS places are established by employing the original map from OpenStreetMap and the software of Mapbox and QGIS. The spatial characters have been presented in Fig. 8, and the detailed descriptions of the data are illustrated as follows.

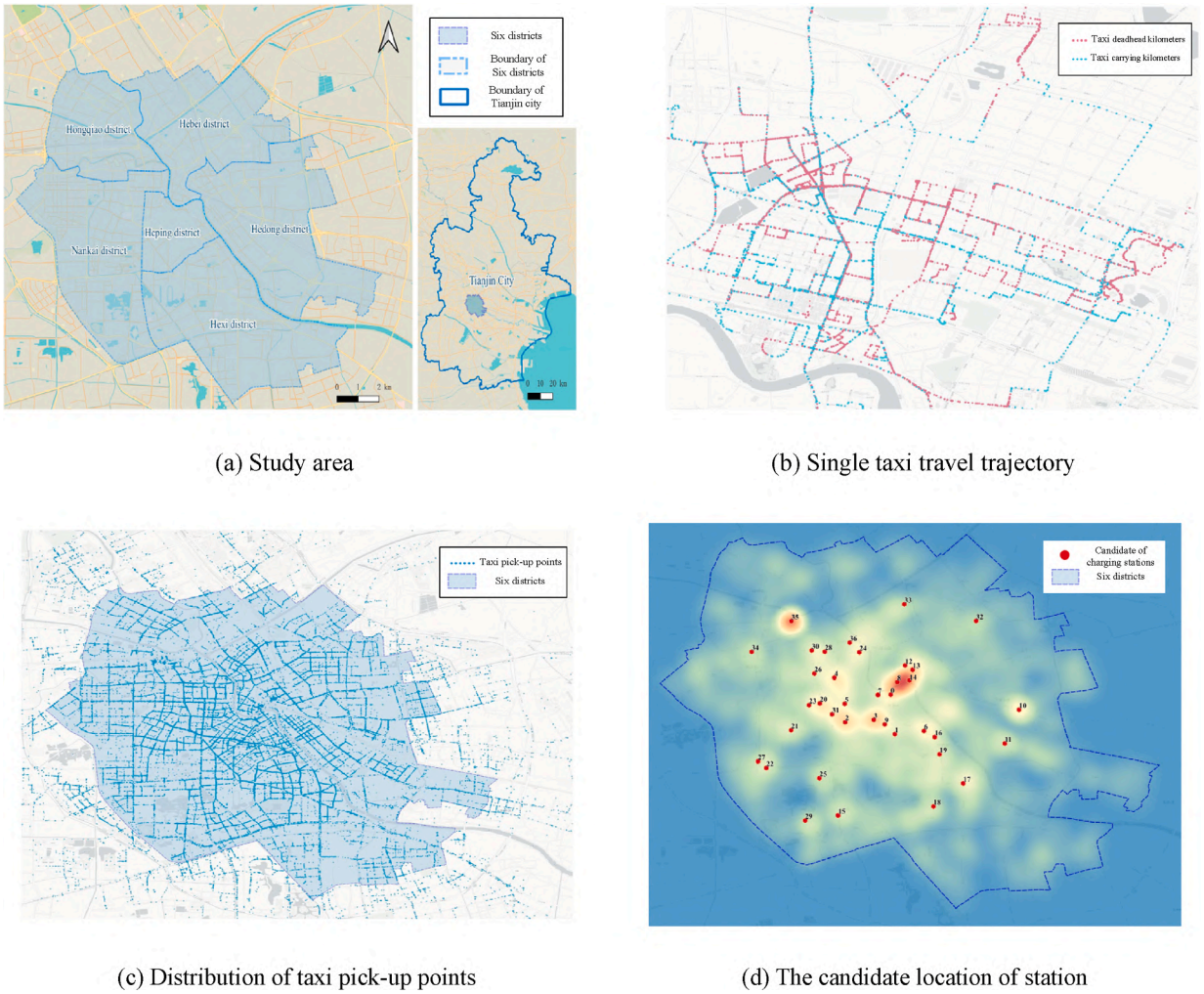

(a) Study area

(b) Single taxi travel trajectory

(c) Distribution of taxi pick-up points

(d) The candidate location of station

Fig. 8. The spatial relationship among urban network, GPS trajectory, taxi demand, and candidate stations.

Taxi GPS data: The raw GPS data was collected from the taxi fleet in Tianjin's six districts on May 22, 2019. The data is transmitted every 10 s with high precision in time and space, including the following effective messages: ID number, working status (where the number 1 indicates the mode of carrying passengers, and 0 represents other modes), longitude, latitude, speed (m/s), and timestamp (s). In total, there are 36,283,834 trajectory records involving 9862 vehicles. The daily taxi trajectory message with order requests has been extracted through the preprocessing of data cleaning, working status recognition, and vehicle trip aggregation. As illustrated in Fig. 8(b), the single taxi travel trajectory is divided by the working status. Additionally, Fig. 8(c) presents the spatial distribution of pick-up points. The density of pick-up points is used to reflect the popularity of passenger demand.

The battery swapping taxi: BAIC EU300, the most popular BST in China, is selected as the research vehicle in the present investigation. Under the new European driving cycle (NEDC) working conditions, the driving range is 300 km, and the battery capacity is 41.4 kWh.

The candidate place of BSS: From the perspective of taxi operations, taxis do not swap batteries while carrying passengers. Subsequently, the drop-off points with high popularity demand are selected as candidate places for BSS. Using Density-Based Spatial Clustering of Applications with Noise (DBSCAN) (Wang et al., 2015), there are 37 clusters, and their centroid points are taken as the suitable candidate place for BSSs, as presented in Fig. 8(d).

The multi-level battery swapping facilities: Based on BSSs broadly utilized by Aulton today, the level 1 BSS and level 2 BSS refer to Aulton 3.0 and Aulton 4.0, respectively. The facilities of the BSS include the swapping robot, swapping batteries, and charging compartments of depleted batteries, with the detailed configuration displayed in Table 4. So the unit decade construction costs of level 1 BSS and level 2 BSS in order are set equal to 4.85 million RMB and 9.05 million RMB. In addition, the charging speed is set as $cs = E/2h$.

Parameter setting of optimization scenario: The simulated period is 24 h, that is, $[0, T] = [0, 86400\ \text{s}]$, where the time slot is one second. The minimum remaining mileage is set equal to 30 km. The initial SOC follows a random distribution of [60 %, 70 %]. In the GA simulations, crossover and mutation probability are set equal to 0.7 and 0.1. Moreover, the population size is 50, and the number of iterations is set as 100. The construction cost of basic scenarios is also set as 55 million RMB. The experiment is tested on a personal desktop with Intel(R) Core (TM) i7-8650U CPU @ 1.90 GHz.

5.2. Results of the basic scenario

(1) The best-found layout

The optimal layout in the basic scenario is shown in Fig. 9 and Table 5. There are 12 BSSs of level 2 and 0 of level 1, with a total construction cost of 72.4 million RMB.

The city center, a cluster providing public social services, including medical care, transportation, and entertainment, is a hot area for taxi order generation/completion. Therefore, to reduce the detour time between order destination and BSSs, appropriate BSSs are established at sites 9, 13, 20, and 35 with high taxi drop-off popularity. The remaining eight stations are built scattered throughout the six districts to extend the service coverage of the BSS.

(2) Spatio-temporal distribution of energy demands

With the best-found layout of BSS facilities, a total of 4,230 battery swapping demands are produced per day. There are 4063 taxis involved, of which 167 vehicles make energy demand twice. The distribution characteristics of energy demands have been displayed in Fig. 10.

Fig. 10(a) shows the distribution of the SOC when the taxis make swapping demands. About 75 % of drivers swap the battery with 25 %–32 % SOC, while only 7 % tolerate continuing driving when the SOC is below 20 %. Fig. 10(b) presents the energy demands aggregated in 1 km * 1 km square grids by rasterizing the grid for the aforementioned six districts. As can be seen in this figure, the popularity of energy demands in the city center is substantially higher than that in the surrounding area.

5.3. Optimal results under various construction costs

In this section, the objective is to choose an appropriate and economical option by making a trade-off between layouts and levels of

Table 4
Parameters pertinent to the multi-level BSS.

Operation parameters of multi-level BSS (level 1 BSS out parentless, level 2 BSS in parentless)			
The number of swapping robots	1 robot (2 robots)		
The number of batteries	28 pieces (56 pieces)		
Operational time	180 s (120 s)		
Land size of swapping station	67.5 m^2 (unknown, assume 90 m^2)		
Price and life of facilities			
Land use price	20,000 RMB/ m^2	Land use life	50 years
Swapping robot price*	450,000 RMB	Swapping robot life*	10 years
Battery price*	38,154 RMB	Battery life	10 years
charging compartments*	113,625 RMB	charging life *	10 years

Note: The price and life with * are from (An et al., 2020), where the Australian dollar exchange rate to RMB is 4.5. The land use price is estimated by the land purchase price in Tianjin.

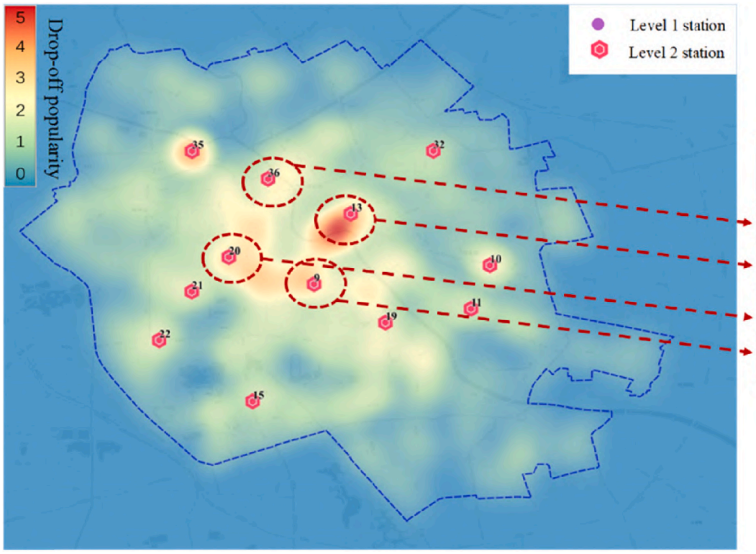

Hot Regions	Types
Tianjin west railway station	Railway station
Tianjin Railway Station	Railway station
Nankai Hospital, Nankai Park	Hospital, Park
Wudadao Urban Historic Conservation Areas	Tourist attraction

Fig. 9. The spatial distribution of best-found solution of BSS layout.

Table 5
The best-found solution of BSS layout.

Indicators	Description
Location of level 1	—
Location of level 2	9,10,11,13,15,19,20,21,22,32,35,36
The sum of level 1 stations	0
The sum of level 2 stations	12
Cost (1 million RMB)	72.4

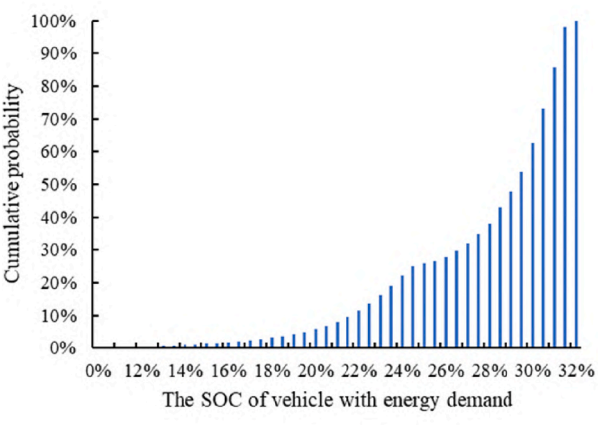

(a) The SOC distribution of vehicle with energy demand

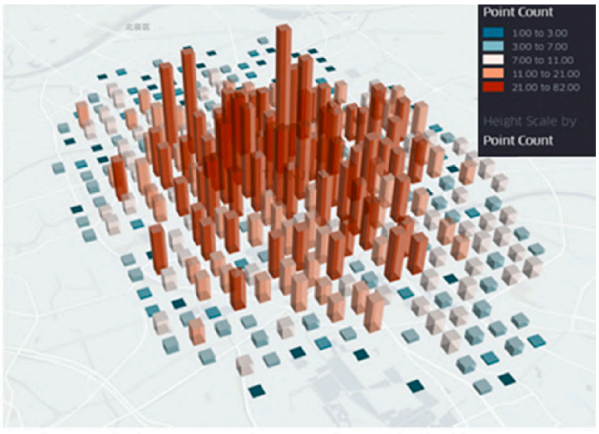

(b) The popularity of energy demands

Fig. 10. The special-temporal distribution of energy demand.

BSS of service, BST's transport capacity, and environmental efficiency. Six scenarios are taken into account, in which their corresponding construction costs are assumed to be 75, 90, 110, 145, 180, and 215 million RMB.

(1) Optimal deployments.

The optimal spatial layouts for various scenarios are presented in Table 6 and Fig. 11. There is a strong positive correlation between the centralization of BSS distribution and the popularity of taxi drop-off demand. When expanding the scale of the BSS layout, some candidate sites, such as 10, 15, 17, 18, 19, 22, 32, and 35, are then frequently selected because of their unique geographical locations. In the cases of low-cost construction (i.e., scenarios 1, 2, & 3), the level 2 BSS with higher service capacity is preferred to be

Table 6
The optimal infrastructures in various construction costs.

scenario	Cost	Location of level 1	Location of level 2	Sum[1]	Sum[2]
1	72.4	—	10,12,15,17,19,20, 22,30	0	8
2	90.5	—	3,10,11,14,18,19,22, 29,34,35	0	10
3	109.2	—	9,10,11,13,15,19,20, 21,22,32,35,36	0	12
4	141.9	5,6,19	3,10,11,13,15,17,18, 23,24,27,32,33,34,35	3	14
5	178.9	1,22,25,26,29	5,9,10,11,12,15,16,17,18,21,27,30,32,33, 34,35,36	5	17
6	212.3	2,5,16,19,21,22,23, 26,31,36	0,3,6,10,11,12,15,17, 18,20,24,27,28,29, 32,33,34,35	10	18

[1] The sum of level 1 stations.
[2] The sum of level 2 stations.

constructed. With the further growth in construction costs, the level 1 BSS is constructed as a supplement.

(2) The swapping loss time of the BST

The primary concern of BST drivers is the length of swapping loss time, which reflects the impact of the BSM on their original daily operation. The variation trends of the lost time in the presence of various scenarios have been illustrated in Fig. 12, including the swapping loss time, its specific waiting time, and detour time.

Due to the limitation of the number of stations in the preliminary scenarios, the waiting time is the main factor affecting taxis' original operation. In scenario 1, the average waiting time is up to 37.71 min. With the improvement of the BSS network scale, the waiting time is intensely lessened. Once the number of level 2 BSSs grows from 8 to 12, the average waiting time remarkably descends to 0.26 min. With the further expansion of the construction scale, the LOS of the BSS system gradually tends to be stable. The detour time turns out to be the main component of swapping loss time but only ranges from 3 to 4 min.

It should be noticed that the maximum reduction rates of waiting time and detour time are not simultaneously achieved. While the layout scale is altered from scenario 1 to scenario 2, the average waiting time reduces by 88.4 %. In scenario 4, the average detour time reduces by 14.3 % compared with scenario 3 due to the supplemental construction of level 1 BSSs. It is because the waiting time is influenced by the service capacity of the BSS, while the detour time relies on the density of the BSS layout.

(3) The LOS of the BSS system

To evaluate the LOS of the BSS system, four indicators are introduced, namely the number of services, the average waiting time, the maximum queue length, and the maximum waiting time. The results of the BSS systems in six scenarios have been presented in Table 7.

Under the same layout, the level of BSS noticeably influences the service capacity as the average daily number of taxis serviced at level 1 ranges from 10 to 60, while varies between 200 and 300 at level 2. The level 2 BSS with two service robots, exhibits a lower average waiting time in comparison with respect to level 1 when there are far more taxis being serviced in level 1, as demonstrated in scenarios 4–6. Additionally, the expansion in the BSS scale results in an improvement in the service capacity of the whole BSS network. As in scenario 3, the LOS of the BSS system is substantially enhanced compared with scenarios 1 and 2. Its maximum queue length is 4.3, and the corresponding waiting time is 8.9 min, illustrating that the whole BSS system in scenario 3 still provides a high LOS for BSTs at the power consumption peak.

Furthermore, the indicator E^m is introduced to assess the spatial equilibrium of each load exerted on the BSS system. According to Ref. (Yang, et al., 2015), the formulation is given in Eq. (23):

$$E^m = \frac{S(\phi^m)}{B(\phi^m)}$$

where ϕ^m represents the set of the service level parameter m of each station, meaning the number of services. $S(\phi^m)$ and $B(\phi^m)$ stand for the standard deviation and the mean value ofϕ_c^m, respectively. As a general rule, the index E^m approaches zero more, the greater spatial equilibrium of the BSS system's load.

The trend presented in Fig. 13 reveals that the expansion of the infrastructure scale leads to the reduction of the system load equilibrium. The reason is that BST drivers essentially choose BSSs based on their geographical location with the improvement of the BSS service capacity and service level, resulting in an uneven spatial distribution of the swapping demand.

Furthermore, the spatial equilibrium states of the level 1 and level 2 BSS network are compared. The E^m of the level 2 BSS system is less than 0.15 in scenarios 1–6, indicating that the daily workload of each BSS network is more evenly distributed spatially. Compared with the level 2 BSS system, the load distribution of level 1 is extremely uneven, with E^m around 0.4 in scenarios 5 and 6. The level 1 BSS, as an auxiliary BSS, attracts load chiefly depending on its geographical location, leading to spatially uneven load distribution. While the battery swapping demand is more equilibrated in the level 2 BSS system due to the larger service coverage and attraction intensity.

(4) Transport capacity of the taxi industry

From the perspective of the taxi industry, it is concerned about how its transport capacity could be affected by the BSM. Hence, the

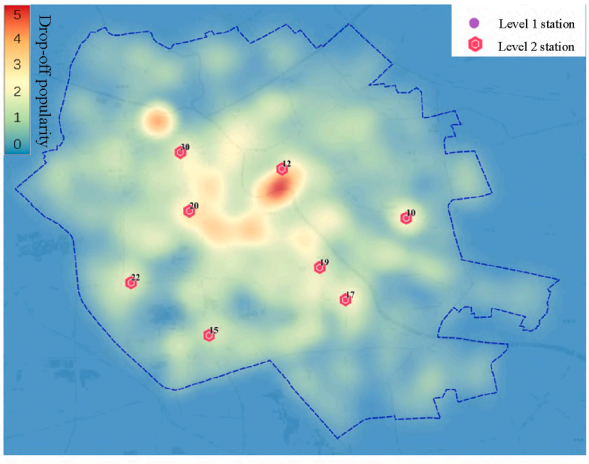

(a) layout of scenario 1

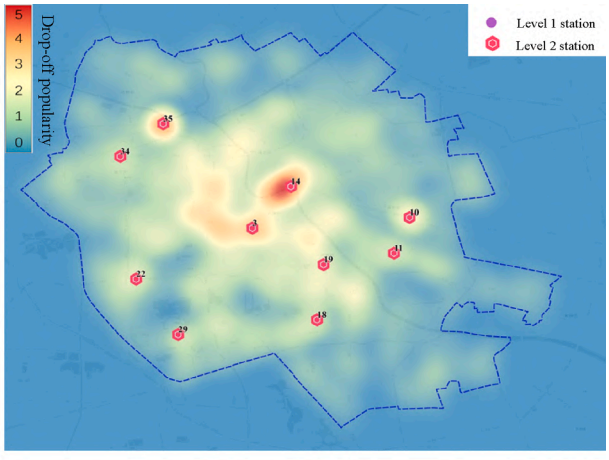

(b) layout of scenario 2

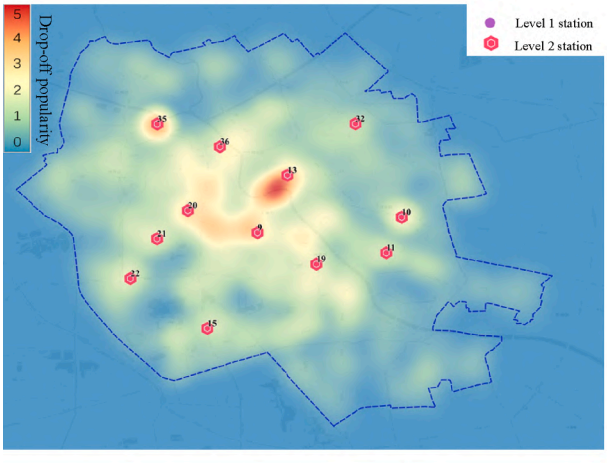

(c) layout of scenario 3

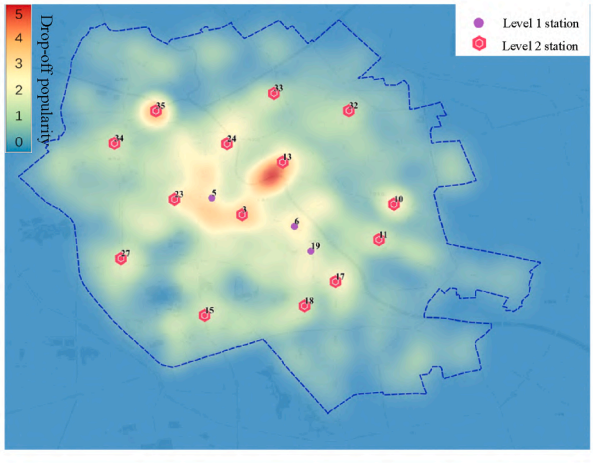

(d) layout of scenario 4

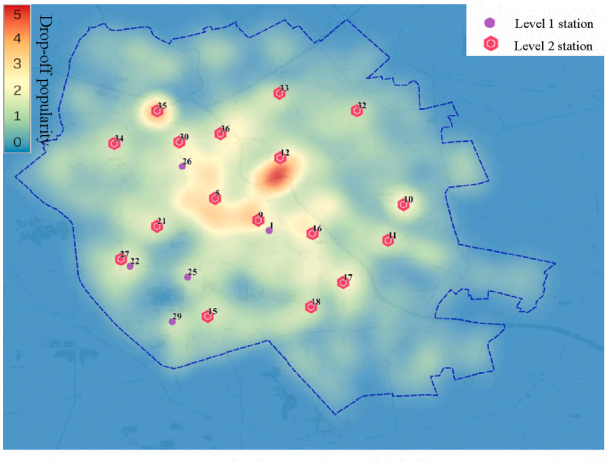

(e) layout of scenario 5

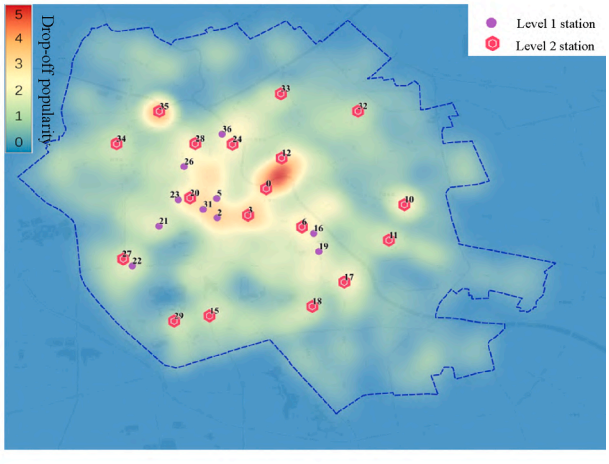

(f) layout of scenario 6

Fig. 11. The optimal layouts of BSS under different construction costs.

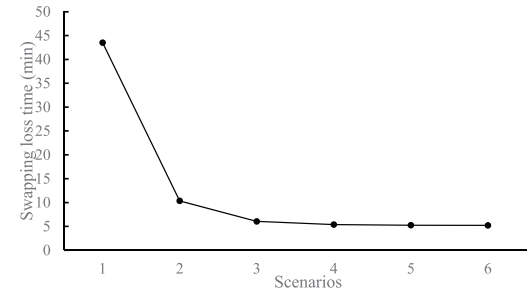

(a) The trend of average swapping loss time

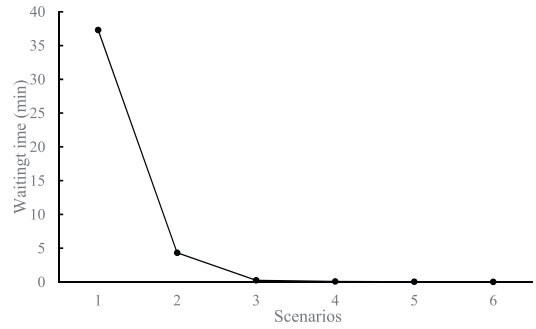

(b) The trend of average waiting time

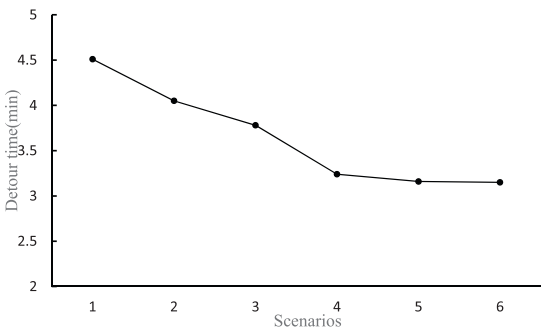

(a) The trend of average detour time

Fig. 12. The average swapping time of BST under different construction scenarios.

Table 7
The service capacity of BSS system in various scenarios.

	Level 2 Scenario 1	Level 2 Scenario 2	Level 2 Scenario 3	Level 1 Scenario 4	Level 2 Scenario 4	Level 1 Scenario 5	Level 2 Scenario 5	Level 1 Scenario 6	Level 2 Scenario 6
Number of services	529	423	353	55	290	25	241	14	227
Avg waiting time (min)	37.3	4.3	0.3	0.4	0.1	0.2	0.0	0.1	0.0
Max queue length	56.3	17.1	4.3	1.3	3.3	0.8	2.9	0.6	2.5
Max waiting time (min)	96.0	37.4	8.9	3.6	2.0	2.2	1.7	0.9	1.5

loss of passenger orders due to battery swapping events is evaluated by the following relation:

$$P^{TC} = 1 - \frac{po^{l}}{po^{o}}$$

in which P^{TC} denotes the percentage of remaining transport capacity of taxis in the swapping mode, po^{0} represents the number of original passenger orders, and po^{l} is the number of unfulfilled passenger orders.

Table 8 presents the daily lost orders of BST in the presence of various BSS layouts. The percentage of lost orders is promptly

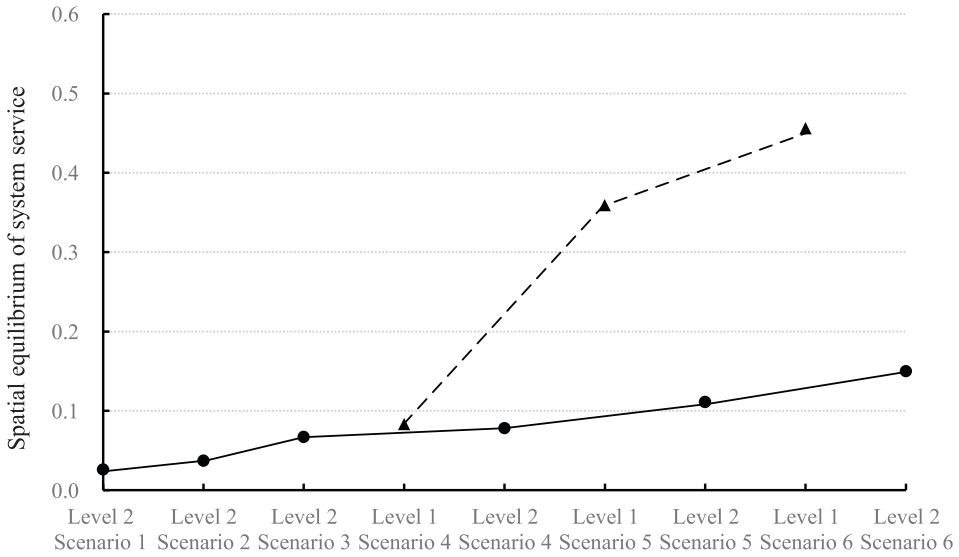

Fig. 13. The spatial equilibrium of BSS system service in various scenarios.

reduced from 7.6 % to 1.9 % from scenario 1 to scenario 3, and the downward trend is gradually weakened after scenario 3. Accordingly, the swapping mode inevitably affects the BST's transport capacity but is acceptable in the presence of a rational layout.

(5) Environmental efficiency

Meanwhile, the government is concerned about the environmental efficiency produced by BSTs. The percentage of the reduced carbon emissions (RCE), denoted by P^{RCE}, is evaluated by:

$$P^{RCE} = \frac{Dis^e * (h^g - h^e)}{Dis^g * h^g}$$

For this equation, the total vehicle CO_2 emissions are calculated by multiplying the travel distance (*Dis*) by the CO_2 emissions factors (*h*). The factors Dis^e and Dis^g in order represent the total travel distance of electric and gasoline vehicles. Based on the carbon emissions calculation method, given in the United Nations Intergovernmental Panel on Climate Change (IPCC), the CO_2 emissions of electric passenger vehicles h^e and gasoline passenger vehicles h^g in order are 19.01 kg/100 km and 34.01 kg/100 km (Wang et al., 2021). In this sub-section, the BSTs with a waiting time of more than 30 min for swapping batteries are considered as gasoline vehicles since their normal taxi operations are seriously influenced.

As presented in Table 8, the BST penetration is swiftly growing from 37.16 % to 99.98 % with the growth of the BSS system in scenarios 1–3. Furthermore, the corresponding daily CO_2 of the BTS grows from 24086.7 kg to 66363.1 kg, and the percentage of the RCE enhances from 16.00 % to 44.09 %. Further, all taxis switch to EV mode in scenario 4, and the percentage of RCE reaches 44.10 %. In conclusion, the layout of BSS under scenarios 2 and 3 ensures the taxi's transport capacity and effect of CO_2 emission reduction, as well as the economy of investment.

(6) Dynamic operational status of station

Furthermore, the daily dynamic operating status of a single station is captured in the proposed multi-agent simulation to examine the mechanism of station congestion generation and dissipation. Fig. 14 displays the second-by-second working status of BSS 10 in scenarios 1–3, including the number of available batteries, queue length, and the minimum waiting time.

Influenced by the spatio-temporal distribution of energy demand, the station's workload noticeably magnifies after 10o'clock. The available batteries are exhausted at 12o'clock in scenario 1. Further, the queue length begins to continuously accumulate from 13:00 to 19:00, then dissipate gradually until 24:00. In scenario 1, the queue congestion process lasts almost 11 h, and the maximum queue

Table 8
The social efficiency of BST under various scenarios.

Indicators	Scenarios 1	2	3	4	5	6
The transport capacity of taxi industry						
Number of lost passenger orders	6242	2290	1539	1407	1399	1380
P^{TC}	7.6 %	2.8 %	1.9 %	1.7 %	1.7 %	1.7 %
The reduced carbon emission						
The percentage of BST	37.16 %	83.97 %	99.98 %	100.00 %	100.00 %	100.00 %
BST daily CO_2 (100 kg)	240.876	557.836	663.631	663.798	663.798	663.798
P^{RCE}	16.00 %	37.06 %	44.09 %	44.10 %	44.10 %	44.10 %

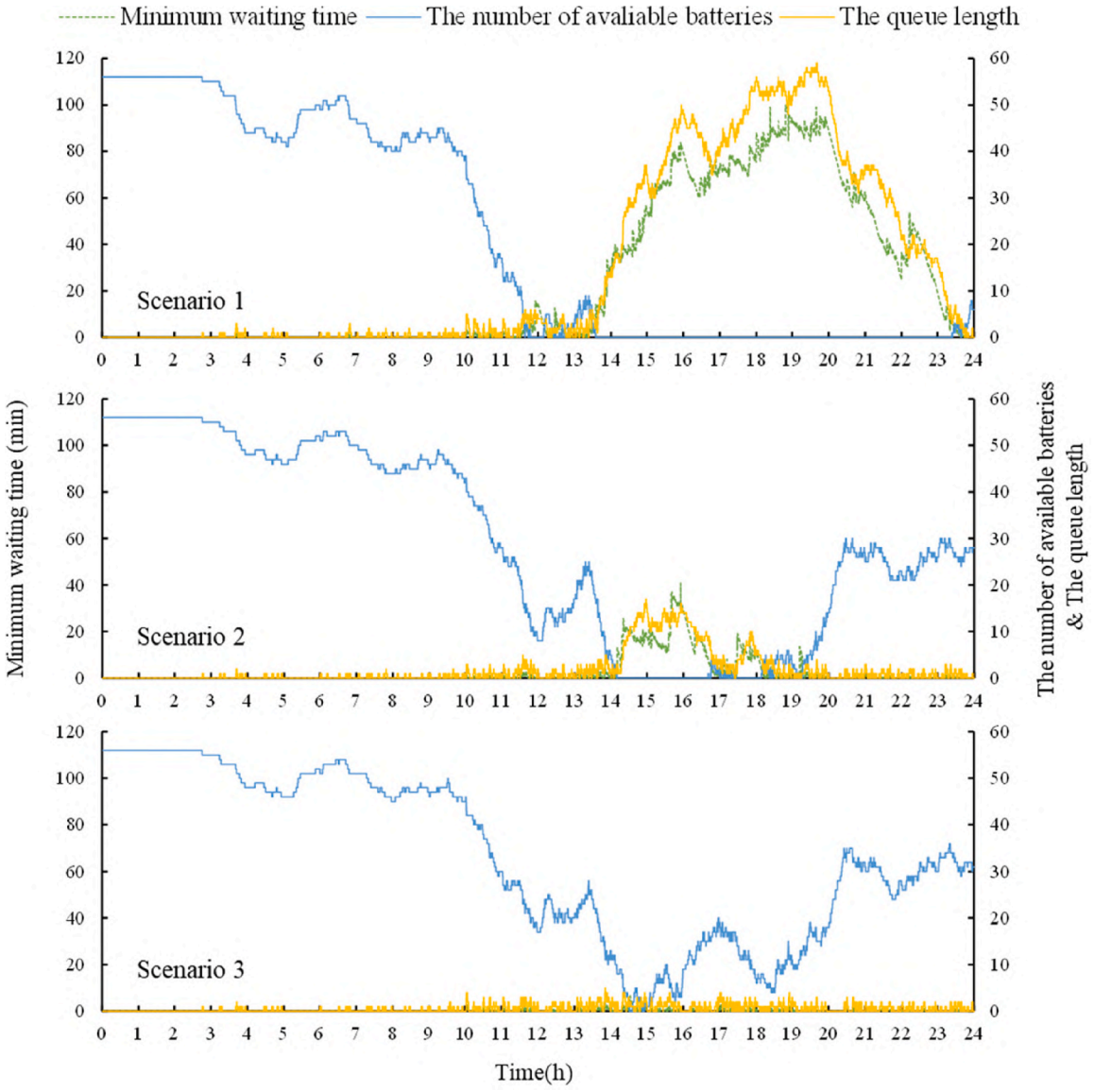

Fig. 14. The daily dynamic operational status of station 10 in scenarios 1–3.

length reaches 58 vehicles. In scenario 2, the LOS of the station has drastically enhanced, where the congestion time lessens to around 3 h, and the maximum queue length is 16 vehicles. In addition, with the expansion of the BSS system layout, no apparent queues for batteries in scenario 3 are detectable. Although there are two troughs in the number of available batteries at 14:30 and 18:00, the available batteries are always provided throughout the day.

In conclusion, considering the BSS system's LOS, the taxi industry's transport capacity, environmental efficiency, and the comprehensively dynamical-operational status of BSSs, scenario 3 is recommended in this case.

5.4. The dynamic simulation efficiency

To verify the efficiency and necessity of dynamic interactions, we compare and examine the system performances in scenario 3 via the proposed BST behavioral model and the shortest path model, which is extensively employed in previous explorations on facility deployment (Jung et al., 2014; Tu et al., 2016).

The corresponding system performances of the above two models are presented in Table 9. In the shortest past model, since drivers always choose the BSS with minimal detour distance, the detour time is only 3.52 min, which is superior to the BST behavior model's results. However, under the proposed BST behavioral model, the average swapping loss time and waiting time are only 6.04 min and 0.26 min, respectively, which are far lower than the obtained results by the shortest path model. This is due to the fact that the driver in

Table 9
The system performance under behavior model and shortest path model.

	Proposed BST behavior model	Shortest path model
The BSS system's LOS		
Swapping loss time (min)	6.04	16.44
Waiting time(min)	0.26	12.92
Detour time(min)	3.78	3.52
The equilibrium of service level	0.067	0.330
The transport capacity of taxi industry		
The percentage of loss passenger orders	1.9 %	3.8 %
The reduced carbon emission		
The percentage of RCE	44.09 %	33.99 %

the BST behavioral model chooses the BSS based on a combination of station geographical location, real-time LOS, and order demand popularity. In addition, the equilibrium of service level is around 0.067 according to the proposed BST behavioral model, while it is predicted to be 0.330 based on the shortest path model. It illustrates that the proposed BST behavioral model establishes a rational information interaction between BST drivers and the BSS network's geographical conditions and real-time working status, thereby improving the BSS systems' service spatial equilibrium. Meanwhile, the percentage of loss passenger orders and the percentage of RCE on the basis of the proposed BST behavior model in order are 1.9 % and 44.09 %, which shows the higher transport capacity and better environmental efficiency compared to those obtained from the shortest path model (3.8 % & 33.99 %).

The above results demonstrate that the dynamic information interactions could provide a BSS system with higher LOS, better spatial equilibrium of service load, higher transport capacity, and more effective emission reduction.

5.5. Sensitivity analysis of technology development

This section aims to assess the impact of technology development on the energy demand of users and the system LOS. On the one hand, the BST's driving range is improved with the battery breakthrough technology. On the other hand, with the development of charging technology, the charging speed of the battery could be enhanced in the near future. Since the BSS system in scenario 1 cannot satisfy the current energy demand of BSTs, which extremely influenced taxi operation, the following takes the BSS layout in this scenario as an example. The corresponding variable settings and detailed analysis are provided as follows.

(1) Sensitivity analysis of the driving range

Considering the development of battery technology in the future, the driving ranges are set equal to 300 km, 350 km, and 400 km. The LOS of respective systems has been presented in Table 10. Several major conclusions are illustrated in the following:

(1) With the increase in the driving range of BST, the whole BSS system's LOS exhibits a sharp improvement. While the driving range grows from 300 km to 400 km, the swapping loss time and waiting time of a single vehicle reduce to about 7.27 min (-83.6 %) and 0.14 min (-99.6 %), respectively.

(2) As soon as the driving range increases, there is a surplus in the service capacity of the BSS system. Compared with the 300 km scenario, the total number of services in the 400 km scenario reduces by 43.8 %. On the one hand, these excess capacities improve the LOS of the system. On the other hand, it could attract new users to choose battery swapping vehicles and expand the BST market.

(2) Sensitivity analysis of the charging speed

As illustrated from the above analysis, the service capacity of the BSS is affected by the robot swapping efficiency and battery charging efficiency. The single operation time of swapping robots in 4.0 mode is only 30 s. Therefore, the charging speed of batteries, which directly affects the battery charging time, is a vital factor limiting the BSS service capacity. To indicate the improvement of charging technology in the future, the charging speed is assumed to be $cs = E/1h$, $cs = E/1.5\ h$, and $cs = E/2h$, respectively.

Fig. 15 demonstrates the dynamic operational status of station 10 at various charging speeds. In the case of $cs = E/2h$, the congested period lasts 11 h from 13:00 to 24:00. When the charging speed enhances to $cs = E/1.5\ h$, the waiting time at station 10 is remarkably lessened, generating congestion at 13:00 and dissipating it completely at 17:00. Furthermore, there are available batteries and no apparent congestion in the station all day in the case of $cs = E/1h$. Once the charging speed increases from $cs = E/2h$ to $cs = E/1h$, the maximum queue length at station 10 experiences a drastical drop from 56 to 6. In the city center, where the land resources are limited and passenger drop-off demands are high, therefore, the charging compartments with faster charging speeds should be equipped to improve the station LOS.

Subsequently, the number of services in each station at various speeds is counted (see Fig. 16). Under the scenario of low-speed charging ($cs = E/2h$), stations 10, 12, and 30 are among the three hot areas, but the charging load of the whole BSS system is moderately balanced. With the enhancement of the charging speed ($cs = E/1.5\ h$, $cs = E/1h$), the choice performance of BST drivers for BSSs becomes more apparent, and the charging load equilibrium of the system reduces. These results reveal that the spatial equilibrium of the system service and charging speed are negatively correlated. For the case of choosing the BSS at a higher charging speed, BST drivers pay more attention to the geographical location of BSSs. Hence, deploying BSS with various charging speeds could adjust the spatial distribution of energy demand to improve the LOS of the whole BSS infrastructure network.

Table 10
Comparison the LOS of Scenario 1 under different driving mileage.

LOS Indicators	Driving range (km)		
	300	350	400
Number of services	4158(0 %)	3759(−9.6 %)	2338(-43.8 %)
Avg charging time of battery (min)	86.98(0 %)	99.03(+13.9 %)	110.53(+27.1 %)
Avg swapping loss time (min)	44.27(0 %)	28.52(-35.6 %)	7.27(-83.6 %)
Avg waiting time (min)	37.95(0 %)	20.85(-45.1 %)	0.14(-99.6 %)
Avg detour time (min)	4.59(0 %)	5.67(+19.0 %)	5.13(+11.8 %)

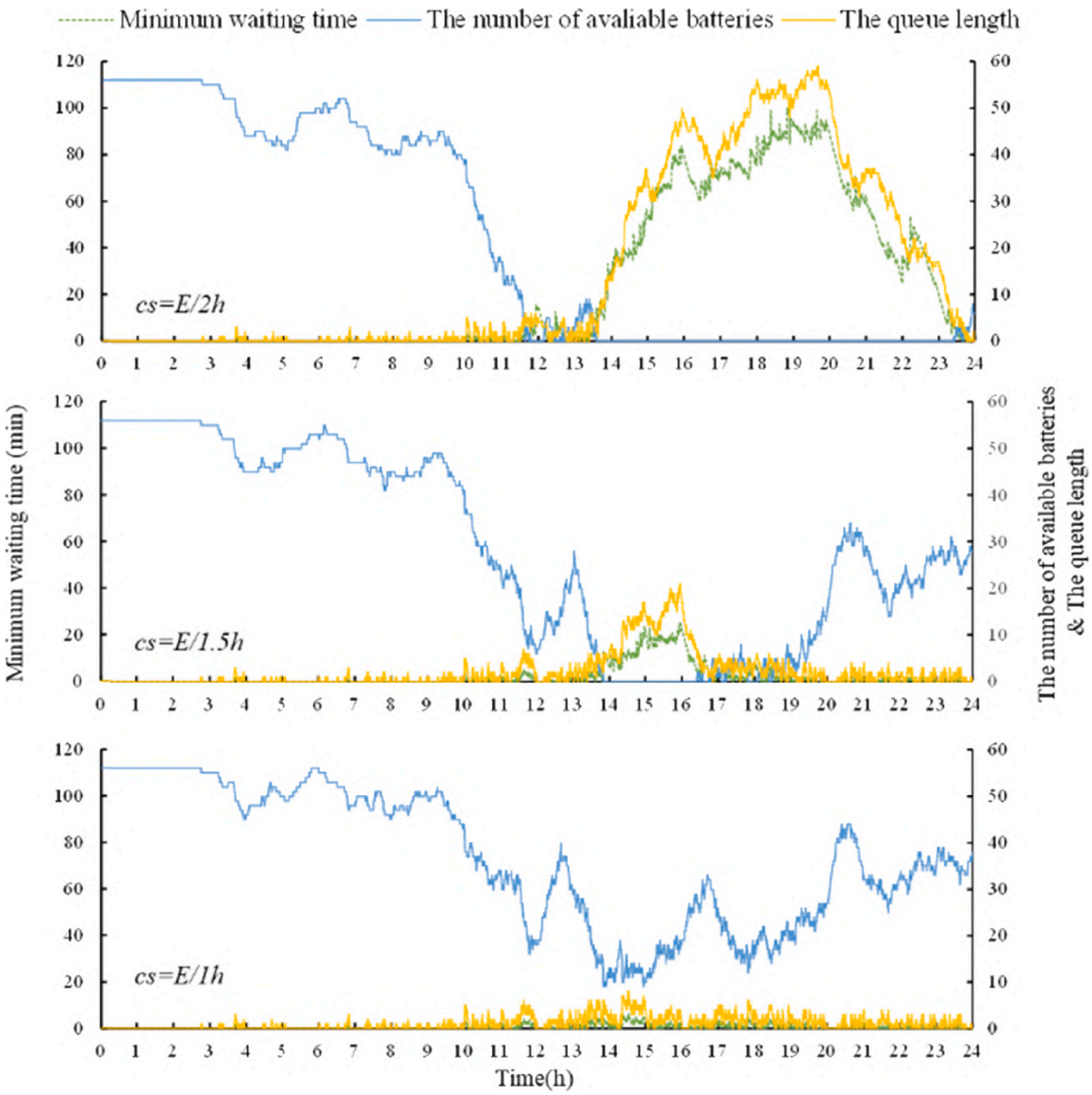

Fig. 15. Dynamic service status of station 10 at different charging speeds.

6. Conclusions and future research

Based on 627 SP samples, the decision-making of swapping demand and BSS choice of BSTs are modeled by the BL and MNL models considering the panel data utility. These models aim to reveal the response mechanism of the energy demand of BST drivers to the driving range, the remaining range, season, swapping price, the number of available batteries, swapping price, queue length, detour

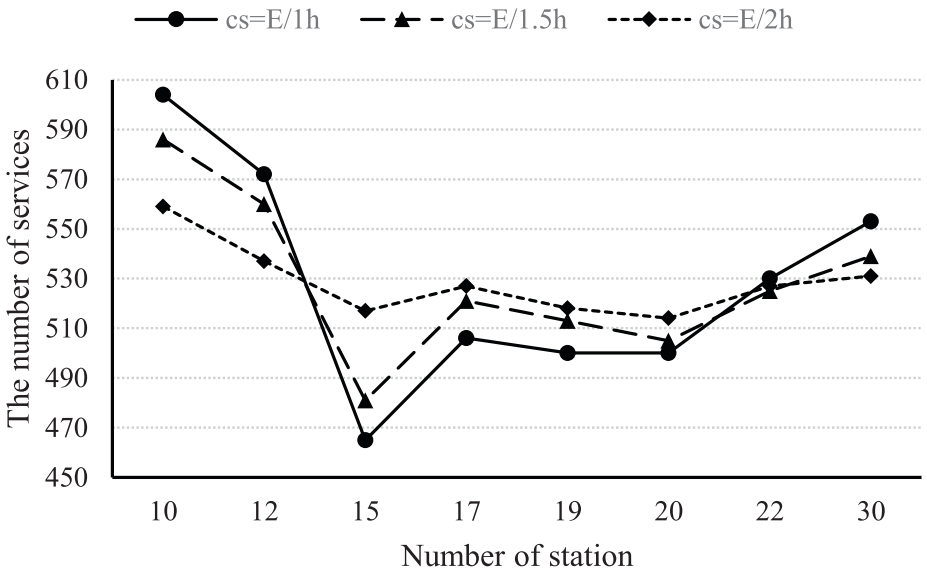

Fig. 16. The spatial distribution of the number of services at different charging speeds.

distance, and the popularity of taxi demand. Based on the proposed MDSDEM, the dynamic swapping demand is also estimated by reconstructing the trip chain of the BST and establishing the dynamic interactions between taxis, passengers, and the BSS network.

Aimed at maximizing the total effective operation time of BST, the multi-level BSS deployment model is proposed to optimize the locations of stations and their corresponding levels. Based on the GPS data involving 9862 taxis, the study is tested in the six districts in Tianjin city of China. Through the evaluation of the BSS deployment's LOS, BST's service capacity, and the environmental efficiency from the perspective of BST drivers, the BSS system, the taxi industry, and the government, the appropriate-economical layout is methodically discovered. In the case of the optimal BSS layout (scenario 3), the taxi industry remains at around 98.1 % of its original capacity and lessens carbon emissions by about 44.09 %. Compared with the shortest path model, the dynamical interactions could reduce orders' loss by about 1.9 % and enhance the BSS network equilibrium from 0.33 to 0.067. Furthermore, sensitivity analyses of the developed driving range and charging speed are provided and discussed. Once the driving range grows from 300 km to 400 km, the number of swapping events decreases by about 43.8 %, providing surplus capacities to attract potential demand. The charging speed of BSSs also plays a vital role in assigning the distribution of energy demand.

There are some limitations to the model developed in this paper. In the near future, the diversified configuration for BSS's facility based on the actual energy demand could be researched to guide the urban BSS deployment. Additionally, it is recommended to explore the orderly deployment schemes of EFCS considering the scenario changes.

Declaration of Competing Interest

The authors declare that they have no known competing financial interests or personal relationships that could have appeared to influence the work reported in this paper.

Acknowledgements:

This research was supported by the General Program of National Natural Science Foundation of China (52172312), the Key Program of National Natural Science Foundation of China (71931003), and the National Natural Science Foundation of China (71801012).

References

Ahmad, F., Saad Alam, M., Saad Alsaidan, I., Shariff, S.M., 2020. Battery swapping station for electric vehicles: opportunities and challenges. IET Smart Grid 3 (3), 280–286.

An, K., Jing, W., Kim, I., 2020. Battery-swapping facility planning for electric buses with local charging systems. Int. J. Sustain. Transp. 14 (7), 489–502.

Ashkrof, P., de Almeida Correia, G.H., van Arem, B., 2020. Analysis of the effect of charging needs on battery electric vehicle drivers' route choice behaviour: A case study in the Netherlands. Transp. Res. Part D: Transp. Environ. 78, 102206.

Aulton., 2021. Battery swapping practice: resource intensive and ecological sharing. https://auto.gasgoo.com/a/70239538.html. (Accessed 29 July 2022).

Bai, X., Chin, x., & Zhou, Z., 2019. A bi-objective model for location planning of electric vehicle charging stations with GPS trajectory data. Computers & Industrial Engineering, 128, pp. 591-604.

Bauer, G.S., Greenblatt, J.B., Gerke, B.F., 2018. Cost, Energy, and Environmental Impact of Automated Electric Taxi Fleets in Manhattan. Environ. Sci. Tech. 52 (8), 4920–4928.

Bogdanov, D., Gulagi, A., Fasihi, M., et al., 2021. Full energy sector transition towards 100% renewable energy supply: Integrating power, heat, transport and industry sectors including desalination[J]. Appl. Energy 283, 116273.
Burnham, A., Dufek, E.J., Stephens, T., Francfort, J., Michelbacher, C., Carlson, R.B., Tanim, T.R., 2017. Enabling fast charging–Infrastructure and economic considerations. J. Power Sources 367, 237–249.
Chaudhari, K., Kandasamy, N.K., Krishnan, A., Ukil, A., Gooi, H.B., 2018. Agent-based aggregated behavior modeling for electric vehicle charging load. IEEE Trans. Ind. Inf. 15 (2), 856–868.
Cilio, L., Babacan, O., 2021. Allocation optimisation of rapid charging stations in large urban areas to support fully electric taxi fleets[J]. Appl. Energy 295, 117072.
ASKCI Consulting Co., Ltd., 2020. Report of National Battery Swapping Station in 2020. https://www.askci.com/news/chanye/20210128/1355581343655.shtml. (Accessed 29 July 2022).
Dong, J., Liu, C., Lin, Z., 2014. Charging infrastructure planning for promoting battery electric vehicles: An activity-based approach using multiday travel data[J]. Transportation Research Part C: Emerging Technologies 38, 44–55.
Gao, Z., LaClair, T., Ou, S., et al., 2019. Evaluation of electric vehicle component performance over eco-driving cycles[J]. Energy 172, 823–839.
He, J., Yang, H., Tang, T.Q., Huang, H.J., 2018. An optimal charging station location model with the consideration of electric vehicle's driving range. Transportation Research Part C: Emerging Technologies 86, 641–654.
Hu, L., Dong, J., Lin, Z., Yang, J., 2018. Analyzing battery electric vehicle feasibility from taxi travel patterns: The case study of New York City, USA. Transportation Research Part C: Emerging Technologies 87, 91–104.
Hu, D., Zhang, J., Zhang, Q., 2019. Optimization design of electric vehicle charging stations based on the forecasting data with service balance consideration. Applied Soft Computing Journal 75, 215–226.
Hu Zhang, T., Boyles, S., & Waller, S. T., 2013. Modeling combined travel choices of electric vehicle drivers with a variational inequality network formulation. Compendium of Papers DVD of TRB 92nd Annual Meeting, Transportation Research Board (No. 13-2619).
Huang, Y., Kockelman, K.M., 2020. Electric vehicle charging station locations: Elastic demand, station congestion, and network equilibrium. Transp. Res. Part D: Transp. Environ. 78, 102179.
Jahn, R.M., Syré, A., Grahle, A., Schlenther, T., Göhlich, D., 2020. Methodology for determining charging strategies for urban private vehicles based on traffic simulation results. Procedia Comput. Sci. 170, 751–756.
Jung, J., Chow, J.Y., Jayakrishnan, R., Park, J.Y., 2014. Stochastic dynamic itinerary interception refueling location problem with queue delay for electric taxi charging stations. Transportation Research Part C: Emerging Technologies 40, 123–142.
Klein, M., Lüpke, L., Günther, M., 2020. Home charging and electric vehicle diffusion: agent-based simulation using choice-based conjoint data[J]. Transp. Res. Part D: Transp. Environ. 88, 102475.
Li, S., Huang, Y., Mason, S.J., 2016. A multi-time optimization model for the deployment of public electric vehicle charging stations on network. Transportation Research Part C: Emerging Technologies 65, 128–143.
Liang, Y., Cai, H., Zou, G., 2021. Configuration and system operation for battery swapping stations in Beijing. Energy 214, 118883.
Ma, F., Yang, Y., Wang, J., et al., 2021. Eco-driving-based cooperative adaptive cruise control of connected vehicles platoon at signalized intersections[J]. Transp. Res. Part D: Transp. Environ. 92, 102746.
MOT (Ministry of Transport of the People's Republic of China)., 2021. China Sustainable Transport Development Report. https://xxgk.mot.gov.cn/2020/jigou/gjhzs/202112/t20211214_3631113.html. (Accessed 29 July 2022).
Nie, Y.M., 2017. How can the taxi industry survive the tide of ridesourcing? Evidence from Shenzhen, China. Transportation Research Part C: Emerging Technologies. 79, 242–256.
Oda, T., Aziz, M., Mitani, T., Watanabe, Y., Kashiwagi, T., 2018. Mitigation of congestion related to quick charging of electric vehicles based on waiting time and cost–benefit analyses: A japanese case study. Sustain. Cities Soc. 36, 99–106.
Pagani, M., Korosec, W., Chokani, N., Abhari, R.S., 2019. User behaviour and electric vehicle charging infrastructure: An agent-based model assessment. Appl. Energy 254, 113680.
Pan, L., Yao, E., MacKenzie, D., 2019. Modeling EV charging choice considering risk attitudes and attribute non-attendance. Transportation Research Part C: Emerging Technologies 102, 60–72.
Rao, R., Cai, H., Xu, M., 2018. Modeling electric taxis' charging behavior using real-world data[J]. Int. J. Sustain. Transp. 12 (6), 452–460.
Sun, X., Yamamoto, T., Morikawa, T., 2016. Fast-charging station choice behavior among battery electric vehicle users. Transportation Research Part D-transport and Environment 46, 26–39.
Tang, B.J., Li, X.Y., Yu, B., Wei, Y.M., 2020. How app-based ride-hailing services influence travel behavior: An empirical study from China. Int. J. Sustain. Transp. 14 (7), 554–568.
The government of China., 2020. 2020 government work report. http://www.gov.cn/zhuanti/2020qglh/2020zfgzbgdzs/2020zfgzbgdzs.html. (Accessed 29 July 2022).
Thøgersen, J., 2006. Understanding repetitive travel mode choices in a stable context: A panel study approach. Transp. Res. A Policy Pract. 40 (8), 621–638.
Tu, W., Li, Q., Fang, Z., Shaw, S., Zhou, B., Chang, X., 2016. Optimizing the locations of electric taxi charging stations: A spatial–temporal demand coverage approach. Transportation Research Part C: Emerging Technologies 65, 172–189.
Wang, M., Wang, Y., Chen, L., Yang, Y., Li, X., 2021. Carbon emission of energy consumption of the electric vehicle development scenario. Environ. Sci. Pollut. Res. 28 (31), 42401–42413.
Wang, W.T., Wu, Y.L., Tang, C.Y., Hor, M.K., 2015. Adaptive density-based spatial clustering of applications with noise (DBSCAN) according to data Vol. 1, 445–451.
Wei, W., Wu, L., Wang, J., Mei, S., 2017. Network equilibrium of coupled transportation and power distribution systems. IEEE Trans. Smart Grid 9 (6), 6764–6779.
World Economic Forum., 2021. Electric taxis and urban fleets can speed decarbonisation - Here's how. https://www.weforum.org/agenda/2021/05/how-urban-fleets-in-madrid-paris-and-lisbon-will-speed-decarbonisation/. (Accessed 29 July 2022).
Wu, H., Pang, G.K.H., Choy, K.L., Lam, H.Y., 2018. An Optimization Model for Electric Vehicle Battery Charging at a Battery Swapping Station. IEEE Trans. Veh. Technol. 67 (2), 881–895.
Yáñez, M.F., Cherchi, E., Heydecker, B.G., de Dios Ortúzar, J., 2011. On the Treatment of Repeated Observations in Panel Data: Efficiency of Mixed Logit Parameter Estimates. Netw. Spat. Econ. 11 (3), 393–418.
Yang, J., Guo, F., Zhang, M., 2017. Optimal planning of swapping/charging station network with customer satisfaction. Transport Res Part E Logist Transp Rev 103, 174–197.
Yang, W., Liu, W., Chung, C.Y., et al., 2020. Joint planning of EV fast charging stations and power distribution systems with balanced traffic flow assignment[J]. IEEE Trans. Ind. Inf. 17 (3), 1795–1809.
Yang, X., Shao, C., Zhuge, C., Sun, M., Wang, P., Wang, S., 2021. Deploying battery swap stations for shared electric vehicles using trajectory data. Transp. Res. Part D: Transp. Environ. 97, 102943.
Yang, Y., Yao, E., Yang, Z., Zhang, R., 2016. Modeling the charging and route choice behavior of BEV drivers. Transportation Research Part C-emerging Technologies 65, 190–204.
Zeng, M., Pan, Y., Zhang, D., Lu, Z., Li, Y., 2019. Data-driven location selection for battery swapping stations. IEEE Access 7, 133760–133771.
Zhang, Y., Guo, H., Li, C., Wang, W., Jiang, X., Liu, Y., 2016. Which One is More Attractive to Traveler, Taxi or Tailored Taxi? An Empirical Study in China. Procedia Eng. 137, 867–875.
Zhang, T.Y., Yang, Y., Zhu, Y.T., Yao, E.J., Wu, K.Q., 2022. Deploying Public Charging Stations for Battery Electric Vehicles on the Expressway Network Based on Dynamic Charging Demand. IEEE Trans. Transp. Electrif. 8 (2), 2531–2548.
Zhou, M., Long, P., Kong, N., Zhao, L., Jia, F., Campy, K.S., 2021. Characterizing the motivational mechanism behind taxi driver's adoption of electric vehicles for living: Insights from China. Transp. Res. A Policy Pract. 144, 134–152.